SIMULATED AND EXPERIMENTAL STUDY OF ANTILOCK BRAKING SYSTEM USING GREY SLIDING MODE CONTROL

by

Yesim Oniz

B.S., Mechatronics Engineering, Sabancı University, 2004

Submitted to the Institute for Graduate Studies in
Science and Engineering in partial fulfillment of
the requirements for the degree of
Master of Science

Graduate Program in Electrical and Electronics Engineering
Boğaziçi University

2007

SIMULATED AND EXPERIMENTAL STUDY OF ANTILOCK BRAKING SYSTEM USING GREY SLIDING MODE CONTROL

APPROVED BY:

Prof. Okyay Kaynak (Thesis Supervisor)	.....
Assist. Prof. Mehmet Akar	.....
Prof. Levent Akın	.....

DATE OF APPROVAL: 21.09.2007

ACKNOWLEDGEMENTS

First and foremost, I would like to express my heartfelt gratitude to my advisor Prof. Okyay Kaynak for his invaluable support, continuous guidance and non-wavering trust in me during the past two years. This thesis would not have been possible without his interest, encouragement and advice. I would also like to thank the members of the committee Assist. Prof. Mehmet Akar and Prof. Levent Akın for their endeavor to review my thesis and to provide valuable comments and suggestions.

My sincere thanks go to my friends at Mechatronics Laboratory Erdal Kayacan, Çisel Aras and Barış Ulutaş for their friendship, support and contributions during the course of this study.

Finally, I want to express my deepest thanks and regards to my family for their never-ending motivation and positive attitude to my academic career. I would like to especially thank my mother, Suheyla Değer, and my spouse Çağıl. Knowing that they were behind me at every decision, inspired me to start my graduate work and kept me going during the hard days.

ABSTRACT

SIMULATED AND EXPERIMENTAL STUDY OF ANTILOCK BRAKING SYSTEM USING GREY SLIDING MODE CONTROL

Antilock Braking System (ABS) is an electronically controlled system that prevents the wheels from locking by limiting the pressure delivered to each slave cylinder of the vehicle. By preventing lock up, ABS gives the driver the opportunity to maintain the steering control of the vehicle during emergency braking.

The main control objective of ABS is to increase the tractive forces between wheels and road surface by keeping the wheel slip at the peak value of road adhesion coefficient vs wheel slip curve. Conventionally, it is assumed that optimal wheel slip is some constant. In this thesis, a grey sliding mode controller is proposed to regulate optimal wheel slip depending on the vehicle forward velocity. The selection of the sliding mode control algorithm is based on the fact that ABS exhibits strongly nonlinear and uncertain characteristics, and to overcome these difficulties, robust control methods should be employed. The concept of grey system theory, which has a certain prediction capability, offers an alternative approach to conventional control methods. The proposed controller anticipates the upcoming values of wheel slip and optimal wheel slip, and takes the necessary action to keep wheel slip at the corresponding optimum value. The control algorithm is applied to a quarter vehicle model, and it is verified through simulations indicating fast convergence and good performance of the designed controller. Simulated results are validated on real time applications using a laboratory experimental setup.

ÖZET

KİLİTLENMEYEN FREN SİSTEMİ (KFS) İÇİN GRİ KAYMA KİPLİ DENETLEYİCİNİN MODELLENMESİ VE TASARIMI

Kilitlenmeyen Fren Sistemi (KFS), alt merkez silindirinin hidrolik basıncını sınırlayarak taşıtın tekerleklerinin kilitlenmesini engelleyen elektronik bir denetim sistemidir. KFS, acil frenleme durumlarında tekerleklerin kilitlenmesini önleyerek sürücünün direksiyon hakimiyetini kaybetmemesini sağlar.

KFS'nin en temel amacı, kayma değerini daima yol tutunma katsayısı-kayma eğrisinin tepe noktasında tutarak yol ve tekerlekler arasındaki sürtünme kuvvetini arttırmaktır. Genellikle en iyi kayma değerinin sabit olduğu varsayılır. Bu tez çalışmasında ise, taşıtın anlık doğrusal hızına bağlı olarak değişen en iyi kayma değerini kontrol etmek amacıyla bir gri kayma kipli denetleyici önerilmiştir. KFS, yüksek derecede doğrusal olmayan elektromekanik bir sistemdir ve belirsizlikler içeren bazı özniteliklere sahiptir. Bu güçlüklerin üstesinden gelebilmek için gürbüz denetim yöntemleri kullanılmalıdır. Öngörüsel yetenek kazandırılmış gri kayma kipli denetleyici, geleneksel denetim yöntemlerine bir alternatif olarak sunulmuştur. Önerilen denetleyici, anlık kayma ve en iyi kayma değerini öngörerek sistemin anlık kayma değerinin hedeflenen en uygun değerde tutulmasını amaçlamaktadır. Geliştirilen denetim algoritması, çeyrek taşıt modeli üzerinde uygulanmış; hızlı yakınsama ve daha iyi başarım gösterdiği benzetim sonuçları ile doğrulanmıştır. Benzetim çalışmalarından elde edilen sonuçlar, deneysel laboratuvar düzeneğinde gerçekleştirilen gerçek zamanlı uygulamalar ile benzerlik göstermektedir.

TABLE OF CONTENTS

LIST OF FIGURES

LIST OF TABLES

LIST OF SYMBOLS/ABBREVIATIONS

D	First order accumulating generator
$\overline{D}$	First order inverse accumulating generator
d_1	Viscous friction coefficient of the upper wheel
d_2	Viscous friction coefficient of the lower wheel
e	System error
F_n	Total normal load
F_t	Road friction force
J_1	Moment of inertia of the upper wheel
J_2	Moment of inertia of the lower wheel
M_{10}	Static friction of the upper wheel
M_{20}	Static friction of the lower wheel
M_g	Moment of gravity acting on balance lever
R	Effective radius of the wheel
r_1	Radius of the upper wheel
r_2	Radius of the lower wheel
$s(x;t)$	Sliding surface
T_B	Braking torque
V	Forward velocity of the vehicle
$V(x)$	Lyapunov function
λ	Wheel slip
λ_R	Reference wheel slip
μ	Road adhesion coefficient
ω	Angular velocity of the wheel
ω_1	Angular velocity of the upper wheel
ω_2	Angular velocity of the lower wheel
$\otimes$	A grey number

ABS	Antilock Braking System
AGO	Accumulating Generating Operation

CGSA	Chinese Grey System Association
ECU	Electronic Control Unit
GM	Grey Model
GSMC	Grey Sliding Mode Controller
IAGO	Inverse Accumulating Generating Operation
PWM	Pulse-width Modulation
SMC	Sliding Mode Controller

1. INTRODUCTION

With the increase in the amount of high speed ground vehicles, safety issues have become increasingly important. Antilock Braking System (ABS), which was initially developed to reduce the stopping distance of airplanes, is currently one of the standard security features offered on most of the newly sold cars because of its capability to help the drivers to stop the car in a shorter distance in the safest way possible.

ABS is an electronically controlled system that helps the driver to maintain control of the vehicle during emergency braking by preventing the wheels from lock up. Once the wheel lock up occurs, the directional stability of the vehicle will be lost and the vehicle cannot be controlled by steering wheel inputs any more, which may result in severe damage and injury. Hence, the primary function of ABS can be stated as to sustain stable vehicle orientation even under conditions such as sudden braking and slippery road surfaces.

Another significant feature of ABS is that by keeping brake pressure just below the point of causing a wheel to lock, ABS ensures that maximum braking power is used to stop the vehicle. This may give rise to shorter stopping distances on slippery or snowy surfaces. However, it is not possible to generalize this situation for every road type, because on very soft surfaces, such as gravel or unpacked snow, ABS may result in even longer stopping distances.

The conventional brake system consists of the brake pedal, master cylinder, brake booster, brake lines, pump, and valves. To stop the vehicle, a greater braking force than the force applied to the pedal by the driver is required. This is achieved by the brake booster, which is located between the brake pedal and master cylinder, using the difference in atmospheric pressure and manifold vacuum of the engine. By depressing the brake pedal causes pressure to be exerted on the booster air valve. Depending on the diameter of the booster diaphragm, a braking force of 2 to 4 times of pedal force is generated and applied to the master cylinder, which is connected to a reservoir

tank filled with hydraulic fluid. As a result of the applied braking force, fluid pressure is created at the master cylinder and it is transmitted to each of the wheel cylinders through brake lines. Hydraulically activated pistons force the shoes and pads into contact with a drum or disc generating friction and converting kinetic energy into heat energy. Figure 1.1 presents a base braking system.

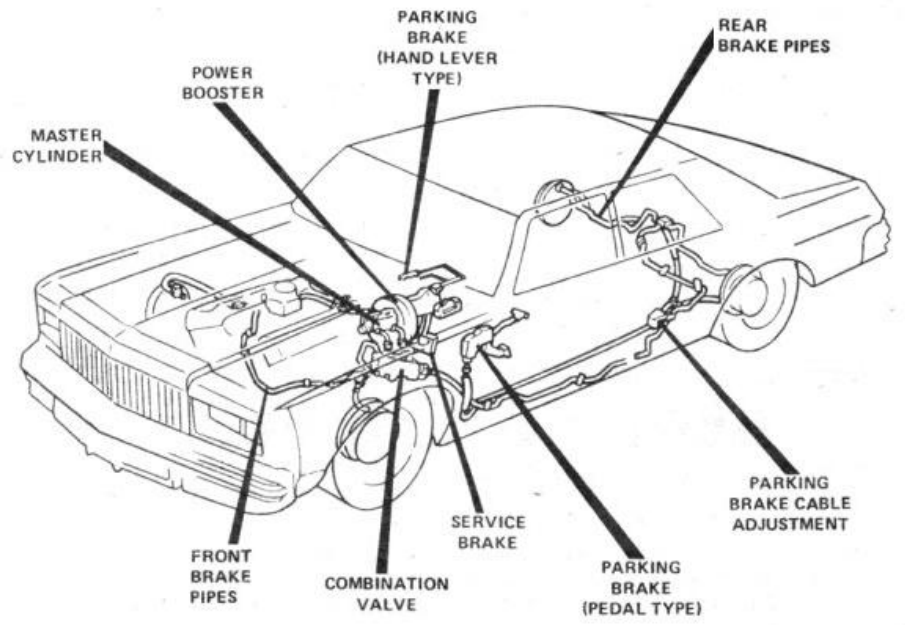

Figure 1.1. Schematic view of a braking system

(Source: http://members.tripod.com/starchief57/techtips.htm)

The ABS system includes all the major components that a conventional brake system has. Additionally, it employs a hydraulic modulator, speed sensors and an electronic control unit (ECU). Figure 1.2 shows the schematic view of an ABS system.

The angular velocity of each wheel and the linear acceleration of the vehicle are measured with sensors. Sensors attached to the wheels send electrical pulses to the ECU at a rate proportional to the wheel speed [1]. The data are used to make the decision whether the wheel is about to lock. If a tendency toward wheel block is perceived, ECU will send signals to the hydraulic modulator and the pressure in the brake cylinder will be reduced. After the wheels are prevented from locking, the

pressure in the cylinder is increased again [2].Regarding the fact that ABS can perform a cyclic application and reduction of braking force at a rate up to 15 times a second, it can be concluded that ABS is much faster and more accurate than a skilled driver can be.

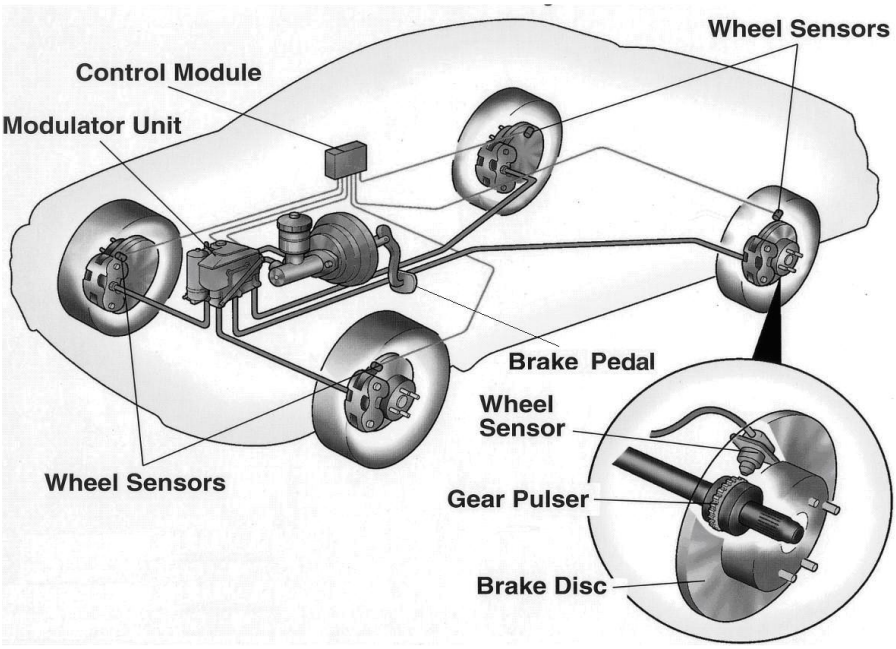

Figure 1.2. Schematic view of an antilock braking system

(Source:http://hdabob.com/ABS.htm)

There are three types of ABS that are commonly used in ground vehicles: [3].

- ***Four-channel, four-sensor ABS***

  This type of ABS is widely used in passenger cars. This is the best configuration available, as there is a speed sensor and a separate valve for each of the four wheels. ABS monitors the velocity of each wheel individually and adjusts the pressure at each wheel to achieve the maximum braking force. Moreover, ABS also compares the angular velocity of each wheel with that of the others, thus avoiding possible risks of loosing control or the turning over of the vehicle. If one of the wheels is rotating at a lower speed, then the pressure in the brake cylinder of that wheel is reduced until all wheels have matching velocities.

- ***Three-channel, three-sensor ABS***

  This ABS configuration is commonly used in pickup trucks. As the name implies, there are three speed sensors and three controlling valves. Each of the front wheels is equipped with a separate speed controller and valve to prevent lock up. However, only one speed sensor and one valve are installed for both of the rear wheels. Since both of the rear wheels are monitored together, for the activation of ABS, they should locked up together. Otherwise, ABS is not activated.

- One-channel, one-sensor ABS

  This is the most basic form of ABS, which makes use of only one speed sensor and one valve. The speed sensor is mounted on the rear axle and the valve controls the pressure at both of the rear wheels. As in three-channel three-sensor ABS, both of the wheels should be locked up for the activation of ABS.

During accelerating or braking, friction forces that are generated between the wheel and road surface are proportional to the normal load of the vehicle. The coefficient of this proportion is called the "road adhesion coefficient" and it is denoted by μ. Studies show that μ is a nonlinear function of wheel slip, which is defined as the measure of relative difference between the vehicle and wheel velocities. λ [4]. The mathematical formula for the wheel slip can be represented as:

$$\lambda = \frac{V - R\omega}{V} \tag{1.1}$$

where V is the forward velocity of the vehicle, ω is the angular velocity of the wheel, and R is the effective radius of the corresponding wheel. While a wheel slip of zero indicates that the wheel velocity and the vehicle velocity are the same, a ratio of one indicates that the tire is not rotating and the wheels are skidding on the road surface; i.e., the vehicle is no longer steerable.

The typical μ-λ curve is obtained from the data of numerous experiments. Most of the ABS controllers are expected to keep the vehicle slip at a particular level, where the corresponding friction force (i.e. road adhesion coefficient) reaches its maximum value.

Zanten states in [5] that the wheel slip should be kept between 0.08 and 0.3 to achieve optimal performance. Furthermore, some research papers show that the reference wheel slip does not have to be a constant value. In [6], the reference wheel slip is considered as a nonlinear function of some physical variables including the velocity of the vehicle.

Although many attempts have been made over the decades, an accurate mathematical model of ABS has not been obtained yet. One of the shortcomings is that the controller must operate at an unstable equilibrium point for optimal performance. A small perturbation of controller input may induce a drastic change in the output. Furthermore at present, there are no affordable sensors which can accurately identify the road surface and make this data available to the ABS controller. Regarding the fact that the system parameters highly depend on the road conditions and vary over a wide range, the performance of ABS may not always be satisfactory. Moreover, sensor signals are usually highly uncertain and noisy [7].

1.1. Literature Review

1.1.1. Historical Overview of ABS

The concept of developing a system to prevent wheel lockup dates back to the beginning of the 20th century. Already, in 1936, Bosch had registered for the patent of a "mechanism to prevent locking of the wheels of a motor vehicle". Although the developed system did not find any acceptance in the industry because of its very complicated and slow structure, it gave rise to research and development projects in the related fields.

Two decades later, in 1952 Dunlop Maxaret ABS, which was a fully mechanical system, was installed in aircrafts for the purpose of shortening the stopping distance [8]. Considering the superiority of this system over conventional brakes, car manufacturers started to seek out ways to adapt ABS to passenger cars. The first automobile with Maxaret-based ABS was the British-made Jensen Interceptor FF built in 1972. There were some other companies which implemented ABS in their models; however early

models of ABS were very expensive and unreliable and hence, they were withdrawn from the market in the middle of the 1970s.

In 1978, Bosch was the first company in the world that developed a modern antilock braking system with electronic control for cars [9]. The developed system was offered in Mercedes Benz's S-class and BMW's 7-series as optional equipment. In the 1990s, ABS was a common option for most of the passenger cars. By the year 1991, one-third of the new vehicles were equipped with ABS. Currently, ABS is a standard or at least optional feature on almost every car and roughly 75 per cent of all vehicles produced worldwide have ABS on board [10].

1.1.2. Control Algorithms

Because of the highly nonlinear and uncertain structure of ABS, many difficulties arise in the design of a wheel slip regulating controller. Consequently, the existing control algorithms for ABS are mostly developed through iterative laboratory experiments, which also attract researchers to find theoretical bases for empirical data.

Almost every control algorithm proposed for ABS utilizes the measured variables such as wheel velocity, vehicle acceleration, brake pressure to estimate actual wheel slip and desired value of wheel slip. The difference between these two variables determines the amount of braking torque that should be applied to the system. Different approaches are taken by the researchers to keep the wheel slip at the desired level.

Among others, sliding mode control is a preferable option to regulate wheel slip, as it guarantees the robustness of the system for changing working conditions. The main idea behind this control scheme is to restrict the motion of the system in a plane referred to as "sliding surface", where the predefined function of error is zero. The stability requirements for the sliding surface are described in [45]. Unlike Tan [12] and Chin [13], who assume that the optimal value of wheel slip resulting in maximum braking torque is known, Drakunov et al. [14] employ sliding mode to achieve the maximum value of friction force without the priori knowledge of optimum slip. In this

study, a simplified four-wheel vehicle without lateral motion is considered and optimal slip is determined using a friction force observer.

Kachroo and Tomizuka proposed a sliding mode controller in [15] that can maintain wheel slip at any desired value, in which they assume that the vehicle and wheel angular velocities can be obtained by direct measurement or estimation. Unsal, et. al. [16] developed a sliding mode controller with a nonlinear observer on a quarter vehicle model to track the reference wheel slip. In this control algorithm, the nonlinear observer estimates vehicle velocity and the controller maintains the wheel slip at the predefined value. Schinkel and Hunt employ, in [17], a sliding mode-like approach for the ABS controller. To deal with the inherently nonlinear dynamics of the vehicle, two uncertain linear systems are employed.

Besides sliding mode control, there are several intelligent control schemes including fuzzy logic control, adaptive control, and neural network approach. Mauer proposed a fuzzy controller in [18] to identify the condition of the road surface. The controller adjusts the braking torque based on the current and past values of wheel slip and brake pressure. Layne et al. [19] also adopted the fuzzy approach and model the plant to be controlled as a first-order linear dynamic system. Will et al. [20] developed a hybrid nonlinear control system that combines the sliding mode based observer with a PID controller. The proposed controller does not require the information of surface type and can compute the optimal value of wheel slip on-line based on the data from longitudinal accelerometers and wheel speed sensors. Lee and Zak [21] have designed an ABS controller using genetic neural fuzzy control. While a neural optimizer is employed to find the optimal wheel slip, the fuzzy component computes the braking torque required to track the optimal slip. A genetic algorithm is used to adjust the parameters of the fuzzy logic component.

1.2. Motivation and Scope of the Thesis

The motivation of this investigation is to propose a sliding mode controller coupled with a grey predictor to track the target value of the wheel slip. Although the

target wheel slip is considered to be a constant corresponding to the maximum value of the road adhesion coefficient in numerous studies, in this thesis, it is taken to be a velocity dependent variable; in other words, as the velocity of the vehicle changes, the optimum value of the wheel slip will also alter. The grey predictor is employed to anticipate the future outputs of the system using current data available. It estimates the forthcoming value of both wheel slip and reference wheel slip; in addition, the sliding mode controller takes the necessary action to maintain wheel slip at the desired value.

This thesis has been organized into seven chapters. Chapter 1 starts with background information on ABS. The working principle and importance of ABS has been explained. Furthermore, an overview of control algorithms for ABS has been provided here. This introductory chapter ends with the statement of objective and scope of the thesis.

In Chapter 2, the laboratory setup of ABS and its components are introduced and the mathematical model is derived. One of the most important features of this setup is its capability of full integration with MATLAB® / Simulink®, which is a software package widely used in the engineering field. Hence, this chapter also explains how to use the software and how to create models of the setup.

An introduction to the sliding mode control is presented in Chapter 3. The underlying idea and mathematics of this control approach are explained. In the subsequent chapter, a sliding mode controller has been designed for ABS and the mathematical equations have been derived. Finally, the simulation and experimental results of ABS for this controller are presented and discussed.

In Chapter 5, grey system theory has been explained. An historical overview of this theory is provided. Next, the design of the grey sliding mode controller has been described. The simulation and experimental results of this controller have been compared with the results obtained by sliding mode controller.

Chapter 6 provides discussion and conclusions of this research.

2. EXPERIMENTAL ABS LABORATORY SETUP

Designing a controller and simulating it in the computer environment can give a general understanding about how the system may behave on an actual system; however, this information is generally neither sufficient nor precise. Because of unpredictable factors such as internal and external disturbances, it is possible that the system may move in an unexpected way, which makes the performance of the proposed control algorithm unacceptable. On the other hand, testing the control algorithms with real full-sized vehicles is a time and cost intensive process. Instead, dynamically similar test systems have been used in place of actual systems to exploit the dynamics and system responses for different controllers.

In this study, the ABS laboratory setup manufactured by Inteco Ltd has been used, which allows precise identification of friction mechanisms and does not require state estimation. The setup shown in Figure 2.1 consists of two rolling wheels. The lower wheel, made of aluminium, imitates relative road motion, whereas the upper wheel, mounted to the balance lever, animates the wheel of the vehicle. The upper wheel has a steel rim covered by a rubber tire. The lower wheel has a smooth surface that can be covered by different materials to animate various road conditions and transition between such conditions.

Figure 2.1. ABS laboratory setup of Inteco Ltd.

As mentioned in Chapter 1, most of the ABS controllers designed throughout history aim to maintain wheel slip at the desired value. This requires accurate measurement of the wheel slip. In this laboratory setup, the angles of rotation of the wheels are measured by two identical encoders. The accuracies of measurements are $2\pi/2048 = 0.175$ degrees. The angular velocities are approximated by differential quotients. We define the car velocity to be equivalent to the angular velocity of the lower wheel multiplied by the radius of this wheel and the angular velocity of the wheel to be equivalent to the angular velocity of the upper wheel. An additional encoder is mounted to the balance lever in order to measure the deviation angle.

At the beginning of an experiment, the lower wheel animating the relative car-road motion should be accelerated to a given threshold velocity. For this purpose, a large flat DC motor is placed on the axle of this wheel. Another DC motor is employed to drive the upper wheel equipped with a disc brake system. Both motors are controlled by pulse-width modulation (PWM) signals of 3.5 kHz frequancy. The relative pulse width of the PWM signal of the upper wheel braking motor is the control variable. When the braking phase begins, the power supply of the big DC motor coupled the lower wheel is switched off to enable the free motion of both wheels.

To communicate with the power interface, a PC equipped with a RT-DAC4/PCI-D multi-purpose digital I/O board is used. The power interface amplifies the control signals which are transmitted from the PC to the DC motor. It also converts the encoder's pulse signals to the digital 16-bit form to be read by the PC. The whole logic necessary to activate and to read the encoder signals and to generate the appropriate sequence of the pulses of PWM to control the DC motor is configured in the Xilinx® chip of the RT-DAC4/PCI-D board. All functions of the board can be accessed from the ABS toolbox which operates directly in the MATLAB® /Simulink® and RTWT toolbox environment.

2.1. Mathematical Model

The free body diagram of the quarter vehicle model describing the longitudinal motion of the vehicle and angular motion of the wheel under braking is presented in Figure 2.2. Although the model is quite simple, it preserves the fundamental characteristics of an actual system. In deriving the dynamic equations of the system, several assumptions have been made. First, only the longitudinal dynamics of the vehicle have been considered, the lateral and vertical motions have been neglected. Furthermore, it is assumed that there is no interaction between the four wheels of the vehicle.

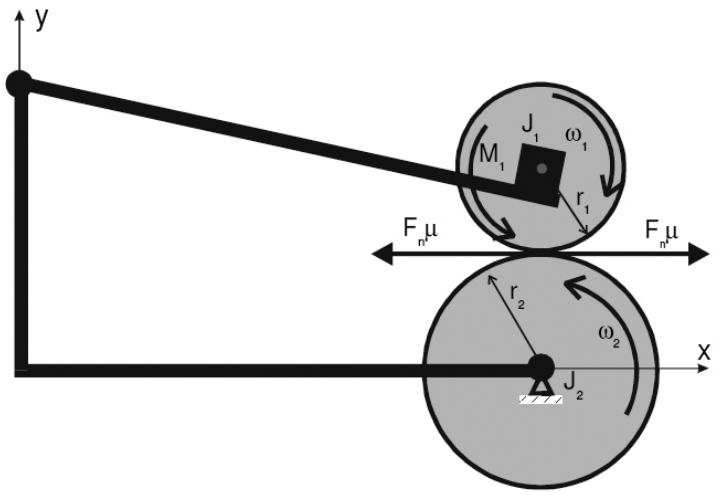

Figure 2.2. Schematic view of ABS laboratory setup

Regarding the model, there are three torques acting on the upper wheel: The braking torque, the friction torque in the upper bearing, and the friction torque among the wheels. Similarly, two torques are acting on the lower wheel: The friction torque in the lower bearing and the friction torque between these wheels.

During deceleration, a braking torque is applied to the upper wheel, which causes the wheel speed to decrease. According to Newton's second law, the equation of the motion of the system can be written as:

Table 2.1. System Parameters

Symbol	**Description**	**Unit**
ω_1	Angular velocity of the upper wheel	rad/s
ω_2	Angular velocity of the lower wheel	rad/s
T_B	Braking torque	Nm
r_1	Radius of the upper wheel	m
r_2	Radius of the lower wheel	m
J_1	Moment of inertia of the upper wheel	kgm^2
J_2	Moment of inertia of the lower wheel	kgm^2
d_1	Viscous friction coefficient of the upper wheel	kgm^2/s
d_2	Viscous friction coefficient of the lower wheel	kgm^2/s
F_n	Total normal load	N
μ	Road adhesion coefficient	
λ	Wheel slip	
λ_R	Reference slip	
F_t	Road friction force	
M_{10}	Static friction of the upper wheel	Nm
M_{20}	Static friction of the lower wheel	Nm
M_g	Moment of gravity acting on balance lever	Nm
L	Distance between the contact point of the wheels and the rotational axis of the balance lever	m
φ	Angle between the normal in the contact point and the line L	^{o}
u	Brake control input	

$$J_1\dot{\omega}_1 = F_t r_1 - (d_1\omega_1 + M_{10} + T_B) \tag{2.1}$$

$$J_2\dot{\omega}_2 = -(F_t r_2 + d_2\omega_2 + M_{20}) \tag{2.2}$$

F_t in Equations (2.1) and (2.2) stands for the road friction force which is given by Coulomb Law:

$$F_t = \mu(\lambda)F_n \tag{2.3}$$

To derive the normal force in Equation (2.3), the sum of torques corresponding to the Point A in Figure 2.3 should be written don. In this figure, L is the distance between the contact point of the wheels and the rotational axis of the balance lever and ϕ is the angle between the normal in the contact point and the line L.

$$F_n L(\sin\varphi - \mu(\lambda)\cos\varphi) = d_1\omega_1 + M_{10} + T_B + M_g \tag{2.4}$$

$$F_n = \frac{d_1\omega_1 + M_{10} + T_B + M_g}{L(\sin\varphi - \mu(\lambda)\cos\varphi)} \tag{2.5}$$

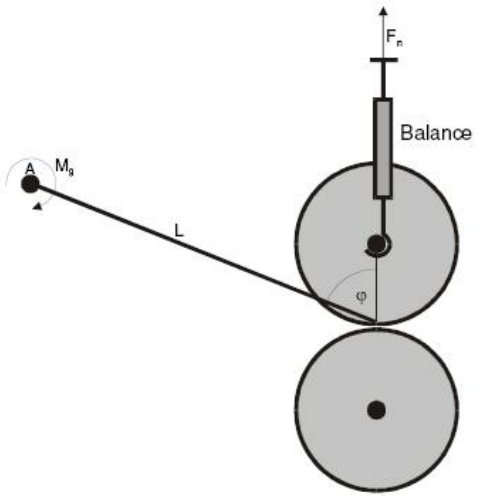

Figure 2.3. Auxiliary diagram to develop the model

Under normal operating conditions, the rotational velocity of the wheel would match the forward velocity of the car. When the brakes are applied, the braking torque is generated which causes the wheel speed to decrease. The braking torque depends on the value of brake control input u, and it can be approximated by the following formula.

$$\dot{T}_B = c_{31}(b(u) - T_B) \tag{2.6}$$

and

$$b(u) = \begin{cases} b_1 u + b_2 & \text{if } u \geq u_0 \\ 0 & \text{otherwise} \end{cases} \tag{2.7}$$

where $c_{31} = 20.37$, $u_0 = 0.415$, $b_1 = 15.24$, and $b_2 = -6.21$. The relationship between the braking torque and brake control input has been presented in the Figure 2.4.

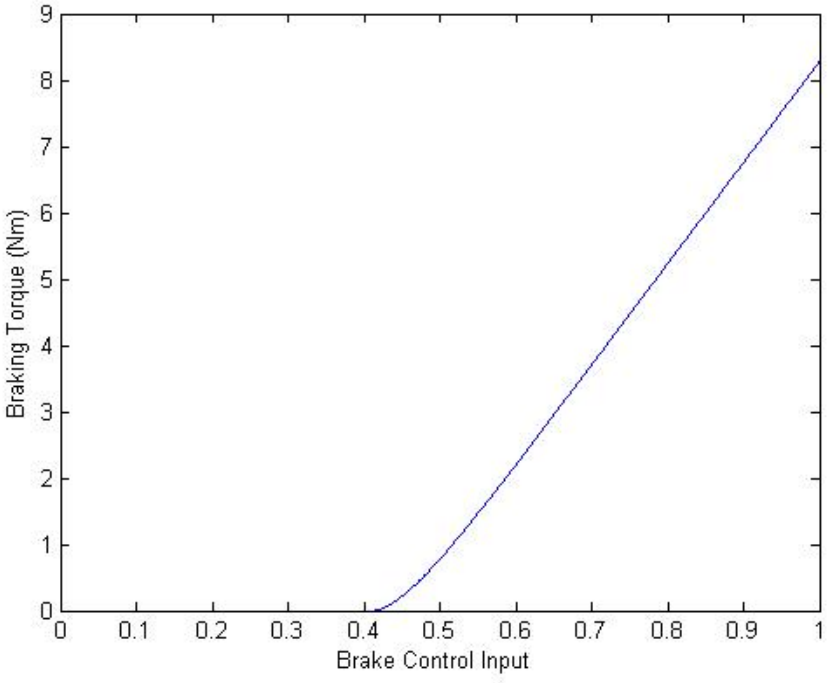

Figure 2.4. Braking torque vs. brake control input

With the application of braking torque, braking forces are generated at the interface between the wheel and road surface. As the force at the wheel increases, slippage will occur between the tire and the road surface, and the wheel speed will tend to be lower than the vehicle speed. The parameter used to specify this difference in these velocities is called "wheel slip" (λ), and it is defined as:

$$\lambda = \frac{r_2\omega_2 - r_1\omega_1}{r_2\omega_2} \tag{2.8}$$

While a wheel slip of *zero* indicates that the wheel velocity and the vehicle velocity are the same, a ratio of *one* indicates that the tire is not rotating and the wheels are skidding on the road surface; i.e., the vehicle is no longer steerable.

The "road adhesion coefficient" (or coefficient of friction) is the proportion of road friction force to the normal load of the vehicle and it is a nonlinear function of some physical variables including wheel slip. There are different approaches to find the value of slip which will maximize the road adhesion coefficient and friction force. In this study, only two of them will be discussed and employed in the designed controllers.

In the first method, it is assumed that the road adhesion coefficient is a single-variable unimodal function of wheel slip. The main issue in this approach is to develop a model to relate wheel slip and the coefficient of friction to each other in such a way that the resulting graph would match with the experimental test results. Figure 2.5 shows the dependence of road adhesion coefficient to the wheel slip based on the experimental results. Furthermore, based on these data, the following formula is derived in [22] to find the road adhesion coefficient corresponding to a wheel slip value.

$$\mu(\lambda) = \frac{c_4\lambda^p}{a + \lambda^p} + c_3\lambda^3 + c_2\lambda^2 + c_1\lambda \tag{2.9}$$

The resulting road adhesion coefficient vs. wheel slip curve is presented in Figure 2.5.

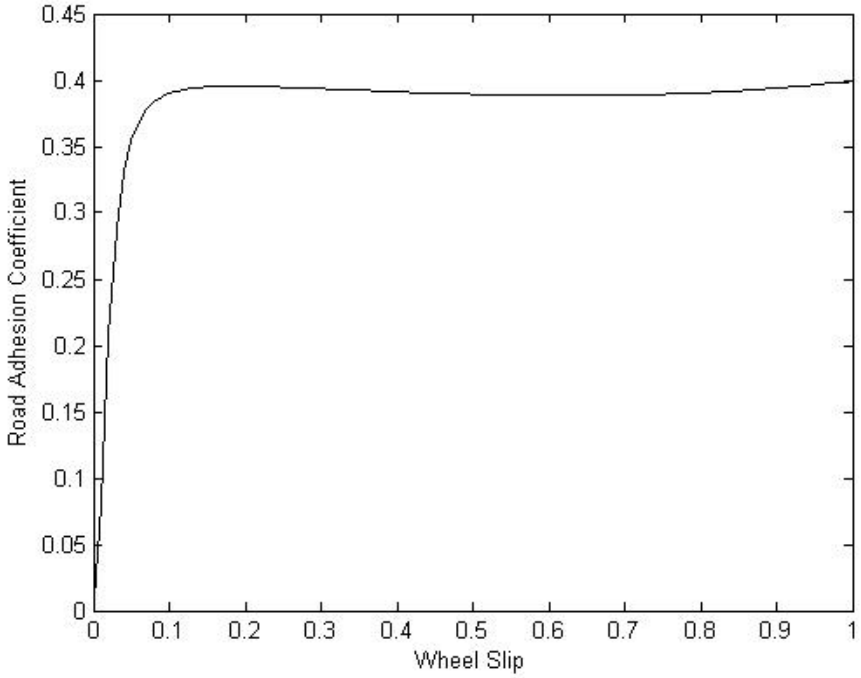

Figure 2.5. Road adhesion coefficient vs. wheel slip

Another approach followed in this study is based on the LuGre dynamic tire/road friction model developed by the Department of Automatic Control in Lund (Sweden) and in Grenoble (France) [23]. This pseudo-static model deals with the dependence of friction on velocity. The following relationship between λ and μ is obtained solving the distributed LuGre tire/road friction model [24].

$$\mu(\eta,\nu) = -h(V_r)\left[1 + 2\gamma\frac{h(V_r)}{\sigma_0 L|\eta|}\left(e^{-\frac{\sigma_0 L|\eta|}{2h(V_r)}} - 1\right)\right] - \sigma_2 V_r \tag{2.10}$$

where $\eta = \frac{\lambda}{\lambda - 1}$, $\quad h(V_r) = \mu_c + (\mu_s - \mu_c)e^{-|\frac{V_r}{V_s}|^{1/2}}$, and $\quad \gamma = 1 - \frac{\sigma_1|\eta|}{Rwh(V_r)}$.

As can be seen from Equation (2.10), if the velocity of the vehicle changes, the curve will change as well. However, the change in the curve will happen faster than a change in the vehicle velocity. Hence, it is possible to calculate the approximated peak value of the braking force produced by tire/road friction for each time step. The description and numerical values or parameters used in this model have been presented in Table 2.2.

Table 2.2. System parameters for LuGre tire/road friction model

Symbol	**Description**	**Value**
L	Length of the tire/road contact patch	0.25 (m)
V_s	Stribeck relative velocity	10 (m/s)
V_r	Relative velocity ($V - R\omega$)	
μ_s	Normalized static friction coefficient	0.5
μ_c	Normalized Coulomb friction coefficient	0.35
σ_0	Rubber longitudinal stiffness	100 (1/m)
σ_1	Rubber longitudinal damping	0.7 (s/m)
σ_2	Viscous relative damping	0.011 (s/m)

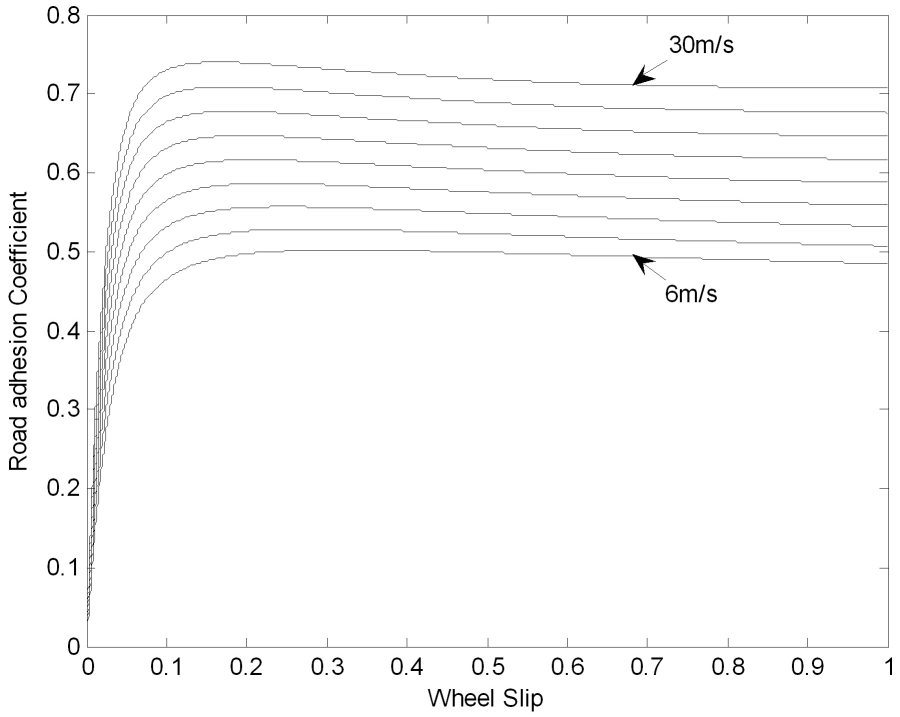

Figure 2.6. μ-λ responses for several velocities

Figure 2.6 shows the relationship between μ and λ for different velocities from 6m/s to 30m/s for every 3m/s increment. The results demonstrate the significant influence of velocity on both the road adhesion coefficient and corresponding slip value.

2.2. Simulation Model

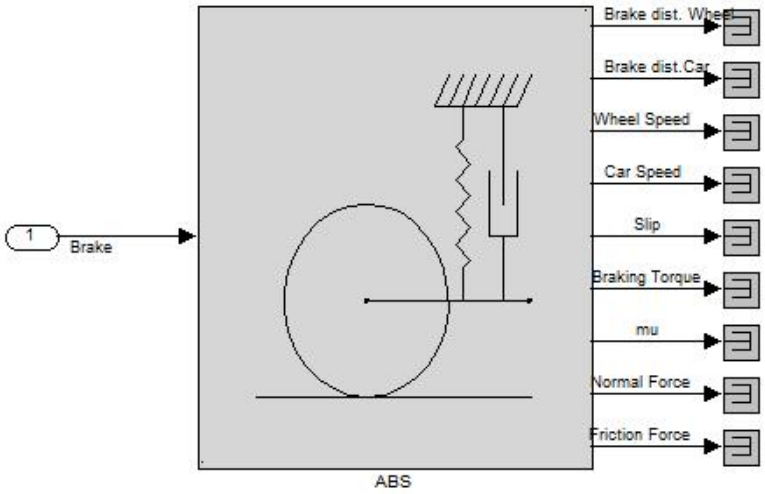

Figure 2.7. ABS simulation model

Earlier in this chapter it was mentioned that the ABS laboratory setup comes with an ABS toolbox operating in MATLAB/Simulink environment. The simulation model included in this toolbox can be used for many purposes such as the design of controllers or the investigation of system responses for different system variables. Figure 2.7 shows the simulation model of the ABS laboratory setup. The control brake input denoted "Brake" is the input of the model and can have values between zero and one. Clicking on the ABS block will produce a window on the screen to allow the user to input the system parameters. When values are entered by the user, an m-file will be executed and outputs of the model will be calculated.

In simulations, there is no need to accelerate the system. The model assumes that the initial velocity is equal to the threshold velocity at which the braking phase will begin. There are nine outputs of the models. These are the stopping distances of car and wheel, wheel and car velocities, slip, braking torque, road adhesion coefficient, normal force, and friction force. Using any of these outputs, the user can design a controller.

Figure 2.8. Mask of the simulation model

2.3. Performing Experiments

The accuracy of the model can be verified by investigating how close the responses of the simulation are to the real system responses. The model used for experiments is more complex than the simulation model. The model of the plant denoted by "ABS" has this time two inputs: Brake and Accelerate. While the vehicle speeds up to reach the threshold velocity, the "Accelerate" input is active. Once the threshold is achieved, the input "Accelerate" will be deactivated and the "Brake" input will be turned on. Figure 2.9 shows the Simulink model used in the experiments.

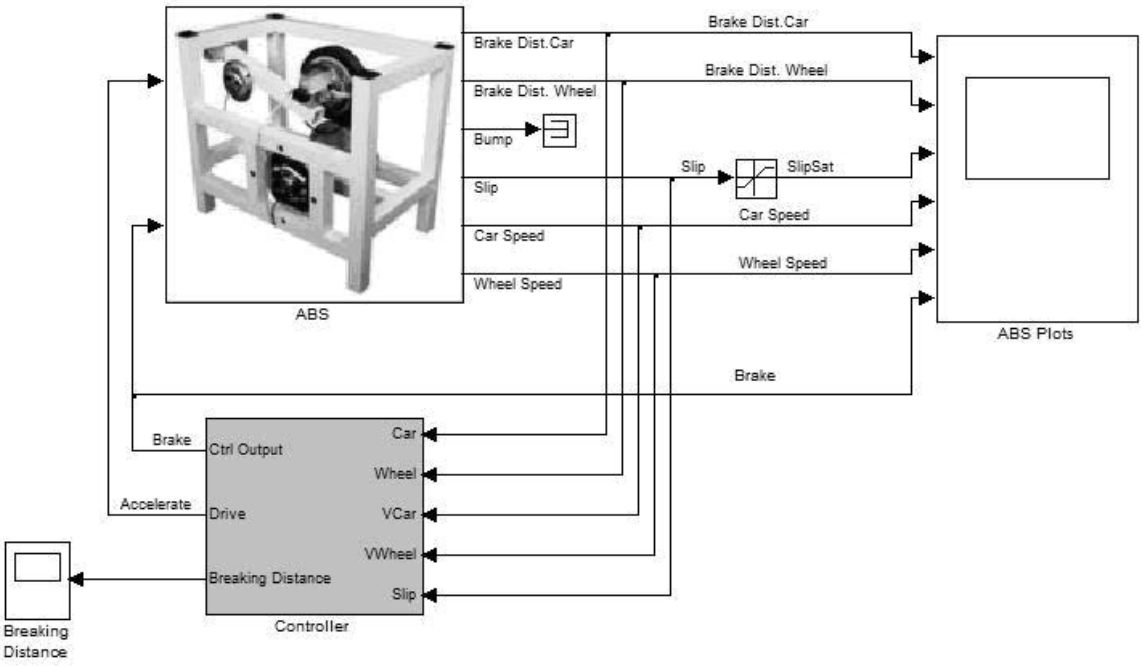

Figure 2.9. ABS control system

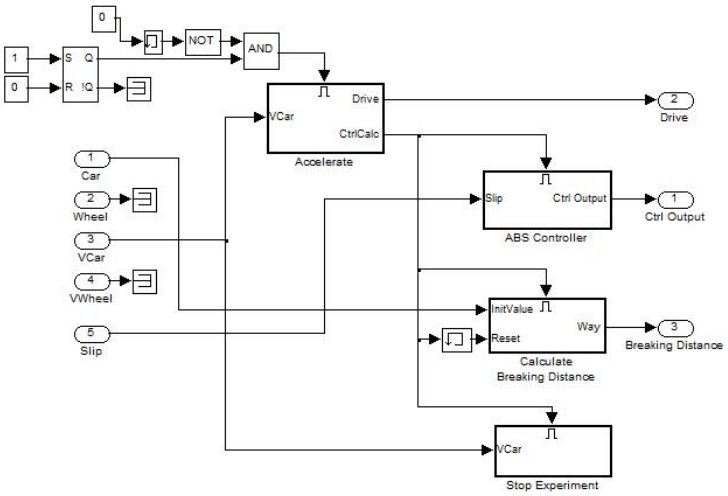

Figure 2.10. Inside of the *Controller* block

The main difference with simulation model is that in simulations, an m-file is used to compute or estimate the outputs of the system; however, in real time experiments, data acquired from sensors are used to determine system outputs. Consequently, experimental model has fewer outputs. For example, F_N is an output of simulation; however, in the experimental model it can not be inferred directly.

To develop the controller of interest, the user should use the interior of the block named “Controller” which is presented in Figure 2.10. As can be seen, there are four subsystems namely Accelerate, ABS Controller, Calculate Braking Distance and Stop Experiment. The names of the blocks correspond to the functions realized by them. For instance, the user should design the controller in the “ABS Controller” block using the information available by the sensor measurements. At the beginning of the experiment, the Acceleration Block is enabled until the predefined velocity threshold is reached. If the Acceleration Block halts, then it will enable the three other blocks. Once the controller is designed, the code for the real time mode should be generated, compiled, linked, and downloaded into the processor. This process requires the selection of a fixed-step solver.

3. SLIDING MODE CONTROL

The imprecision in nonlinear system models may result either from the actual uncertainty about the system such as unknown plant parameters, or from the purposeful choice of a simplified representation of the system dynamics [25]. The vast majority of industrial applications are subjected to disturbances and parameter fluctuations because of the noise in the measurements, mechanical stresses and friction, which can not be computed or estimated beforehand. Moreover, in the derivation of the mathematical model of the plant, several assumptions and linearization can be made to make the calculations easier. These uncertainties can have strong adverse effects on the nonlinear control systems.

Sliding Mode Control is an attractive option to solve problems in nonlinear systems, as it guarantees the robustness of the system for changing working conditions and modeling imprecision. Originating from relay and bang-bang control theory, the main idea behind the sliding mode control is to represent systems described by n^{th}-order differential equations by a differential equation with order one less than the order of the original system. This property of sliding mode control may lead to decoupling and simplification of the design procedure [26]. Consequently, a simple control algorithm that is straightforward and robust can be applied, instead of a complex algorithm.

In sliding mode control, it is intended to drive the state of the system to a predefined sliding (or switching) surface. Once the sliding surface is reached, the system will move on this surface in state space for all subsequent times. A typical sliding mode controller consists of two parts. The first part guarantees the reachability of the sliding surface in finite time. The second part ensures the stability of the motion on the sliding manifold. During the sliding motion operation, the created sliding surface should always direct the state trajectory towards a point where a stable equilibrium point exists. This can be accomplished through the design of the sliding coefficients.

The main drawback of sliding mode control is its switching nature. The discontinuous control action coupled with high gain elements induces high frequency switching. This gives rise to the phenomenon called chattering, which should be reduced for the controller to perform properly.

3.1. Sliding Surfaces

The purpose of sliding mode control is to drive the nonlinear system's states onto a user-defined sliding surface in the state space and to keep them moving along this surface for succeeding times. The rule for switching depends on the position of plant states with regard to the sliding surface and typically there are two different gains for the feedback loop; i.e., when the plant state is above the sliding surface, it has a gain, and it has another gain if the plant's state is below the surface. Once the sliding surface is reached, the system will move along it.

Consider the single input dynamic system

$$y^{(n)} = f(x(t)) + g(x(t))u(t) \tag{3.1}$$

where $x(t)$ is the state vector, $u(t)$ is the control input, y is the output state of the plant, and the superscript n shows the order of differentiation. Furthermore, $f(x(t))$ and $g(x(t))$ present the nonlinear functions of time and states. Their exact values are not known, but the knowledge of their sign and the upper bound for possible uncertainties is available. The main control objective is to make the state y to track the desired time-varying state y_d in the presence of imperfections due to uncertainties involved in $f(x(t))$ and $g(x(t))$. Thus, the most common way to design the sliding surface is given in [28] with the following formula:

$$s(x;t) = (\frac{d}{dt} + \delta)^{(n-1)}(y - y_d) = 0 \tag{3.2}$$

In Equation (3.2), δ stands for a strictly positive constant that represents the bandwidth of the system and $s(x;t)$ is the sliding surface satisfying the equation. As can be seen,

an n-dimensional tracking problem is replaced by a first order stabilization problem in s.

A surface $s(x)$ is attractive if

1. any trajectory starting on the surface remains there
2. any trajectory starting outside the surface tends to the sliding surface at least asymptotically [27]

Thus, a sliding mode will occur if:

$$\lim_{s\to 0^+} \dot{s} < 0 \quad and \quad \lim_{s\to 0^-} \dot{s} > 0 \tag{3.3}$$

The conditions presented above ensure that the motion of system states trajectory x on either side of the sliding surface $s(x) = 0$ is toward the sliding surface. These two conditions can be combined as

$$\dot{s}s < 0 \tag{3.4}$$

which is referred to as the *reachability condition*. Furthermore, to guarantee that the sliding surface will be reached in finite time, the following condition is imposed

$$\frac{1}{2}\frac{d}{dt}s^2 \leq -\eta|s| \tag{3.5}$$

where η is a strictly positive constant. In the literature, this is referred to as the *η-reachability condition* or *sliding condition*.

It can be inferred from Equation (3.5) that the squared distance to the sliding surface, s^2 , decreases along all trajectories and the system states are moving toward the sliding surface s(x;t). Furthermore, once the system states are on the surface, they will remain on it. Equation (3.5) also implies that some disturbances can be tolerated

while still keeping the system states satisfying the sliding conditions. In Figure 3.1 a graphical interpretation is given.

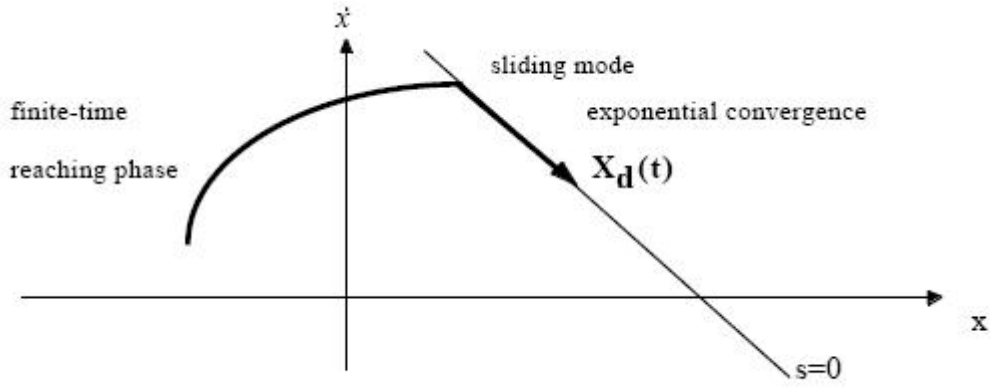

Figure 3.1. Sliding surface for $n = 2$ [28]

If the initial condition of the system is different from the desired state of the system at $t = 0$, Equation (3.5) guarantees that the sliding surface will be reached in a finite time smaller than $s(t = 0)/\eta$. Integrating (3.5) between $t = 0$ and t_{reach} leads to

$$s(t = t_{reach}) - s(t = 0) = 0 - s(t = 0) \leq -\eta(t_{reach} - 0) \tag{3.6}$$

from which t_{reach} can be found as

$$t_{reach} \leq s(t = 0)/\eta \tag{3.7}$$

Equation (3.6) implies that starting from any initial condition the sliding surface will be reached within less than t_{reach}. η is a design parameter that decides the response time of the system. Greater η means that the sliding surface is reached quicker, but it also brings higher control activity.

3.2. Controller Design

The design of the sliding mode controller based on the generalized Lyapunov approach consists of two parts. The first part, which is called the equivalent control, u_{eq}, is a linear control action to maintain the condition $s(x) = 0$ during the reduced

order sliding motion. Since motion in the sliding mode implies that $s(x) = 0$ for $t > 0$, it can be assumed that $ds/dt = \dot{s} = 0$ as well [26]. Hence, equivalent control u_{eq} can be solved from the equation satisfying $\dot{s} = 0$, which keeps the $s(x)$ on the sliding surface. However there exists uncertainties in f and therefore a further discontinuous term,u_h should be added to this to maintain the inequality stated in Equation (3.5).

The overall control law will then have the form:

$$u = u_{eq} - u_h \tag{3.8}$$

Consider the single input dynamic system of the form:

$$\dot{x}(t) = f(t, x) + B(t, x)u(t) \tag{3.9}$$

For controllers having the structure presented above, the following is true [29]

$$\begin{aligned} \dot{s}(t) &= \frac{\partial s}{\partial x}\dot{x} \\ &= \frac{\partial s}{\partial x}\left[f(t, x) + B(t, x)(u_{eq} - u_h)\right] \\ &= \frac{\partial s}{\partial x}\left[f(t, x) + B(t, x)u_{eq}\right] - \frac{\partial s}{\partial x}B(t, x)u_h \\ &= -\frac{\partial s}{\partial x}B(t, x)u_h \end{aligned} \tag{3.10}$$

To check whether the condition stated in Equation (3.3) can be met, let us assume that $B(t, x)$ is equal to the identity. Then, $\dot{s}(x)$ will become equal to $(-u_h)$. In the literature [29] proposed the following structure for the discontinuous control is suggested:

$$u_h = -\alpha sgn(s(x)) \tag{3.11}$$

where $\alpha > 0$, and sgn(s) sets the hitting direction. This controller will meet the

condition stated in Equation (3.3) since

$$s\dot{s} = -s(x)\alpha sgn(s(x)) < 0 \tag{3.12}$$

As can be inferred, the nonlinear components are discontinuous on the individual hyperplanes. In this thesis, this structure will be employed as the discontinuous control. For a more detailed explanation of sliding mode control theory the reader is referred to Reference [26]

3.3. Chattering Reduction

As mentioned earlier, the main idea behind the sliding mode control is to keep the states of the controlled plant satisfying the condition $s(x,t) = 0$ at every $t \geq t_0$ for some t_0. This may require infinitely fast switching, which is unobtainable in real life applications because of the imperfections in the switched controller. The term "chattering" is used to describe the phenomenon of finite frequency, finite amplitude oscillations appearing in many sliding mode implementations [26]. Thus, the desired state or sliding surface will not be reached, but the state of the plant will chatter around it within a neighborhood [30].

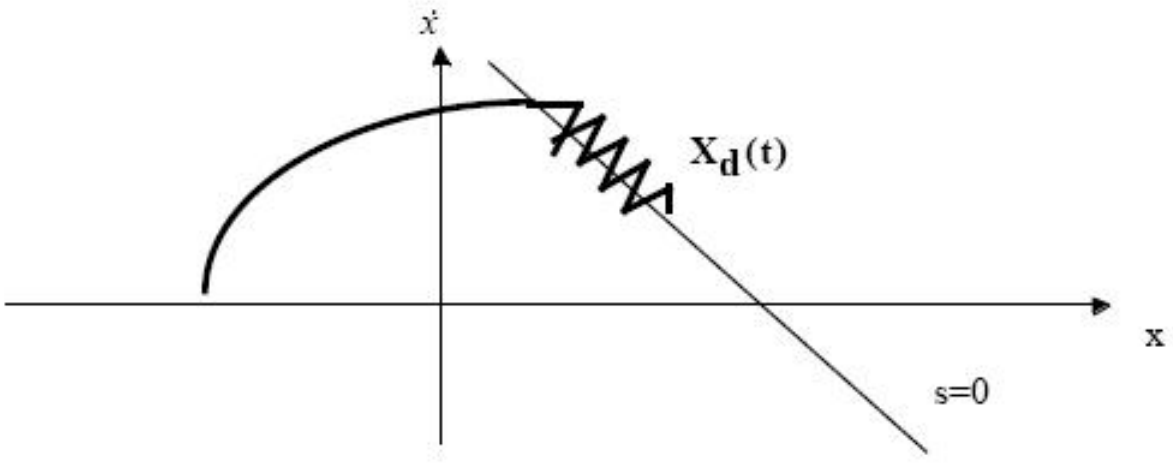

Figure 3.2. The chattering phenomenon [28]

Two main causes of chattering have been identified. The first one is the fast dynamics in the control loop resulting from sensors and actuators, which were neglected in the system model as they are considerably faster than the main system dynamics. These unmodeled dynamics are often excited by the fast switching of sliding mode controllers. Second, the digital implementations in microcontrollers with fixed sampling rates may lead also to discretization chattering [26].

Chattering is highly undesirable in practice as it induces high frequency oscillations, and may degrade the performance of the controller. In some cases, it may even lead to the instability of the system. Fortunately, avoiding chattering does not involve complex mathematics. First, the sliding mode controller can be designed neglecting the effect of the unmodeled dynamics. Then, the discontinuous sign function, $sgn(s)$, in nonlinear control input u_h can be replaced with a continuous approximation [31]. There are different continuous functions employed to reduce chattering. One of the approaches that finds common use is to replace the discontinuous sign function with $\frac{s}{|s|+\phi}$ [32] where ϕ is a positive constant. This is the approach which will be used further in this study. The value of ϕ should be selected very carefully, since for a small value of ϕ, the continuous function curve is close to the $sgn(s)$ curve therefore the control input will have a high gain in the switching surface range and cannot eliminate chattering [34]. On the other hand, a large ϕ may reduce chattering, but the wide boundary layer may cause the system dynamics to become unstable. This is the approach which will be adopted in this thesis.

3.4. Discussions

In this chapter, sliding mode control theory and its underlying mathematics have been presented. The design of the sliding mode controller can be described as a two-step procedure. In the first step, the sliding surface is defined and designed. Following is the determination of the control action which will moves the system onto the sliding surface and keeps it there. Some methods of controller design and two of the continuous functions, which are commonly used instead of the discontinuous function of

discontinuous control to reduce chattering, have been presented and reviewed in this chapter.

The sliding mode controller is an ideal candidate for real time application as it maintains the stability and performance of the systems even in the presence of disturbances and modeling imprecision. Regarding the fact that the vehicle and brake system are highly nonlinear and time-varying systems, in this thesis, a sliding mode controller is employed to regulate wheel slip at any desired value.

4. DESIGN OF SLIDING MODE CONTROLLER (SMC)

Recall from Chapter 1 that ABS exhibits strongly nonlinear and uncertain characteristics. To overcome these difficulties, robust control methods should be employed. Sliding mode control is a preferable option, as it guarantees the robustness of the system for changing working conditions.

During braking, friction forces are generated between the road and tire surfaces, which forces the vehicle to slow down and eventually to stop. The generated force is proportional to the road adhesion coefficient, which is a nonlinear function of some physical variables including wheel slip. Hence, by regulating wheel slip can help to achieve the desired friction force or braking torque. Control algorithms designed for ABS make use of this relation between λ and μ by keeping the wheel slip at the optimum value corresponding to the maximum road adhesion coefficient, i.e. the maximum braking torque and friction force.

The schematic of an ABS controller is presented in Figure 4.1. In this chapter, a sliding mode controller (SMC) based on the Lyapunov stability approach is designed to regulate the wheel slip. The proposed control algorithm has been verified through simulations indicating fast convergence and good performance. Moreover, simulated results have been validated on real time applications using laboratory setup of ABS.

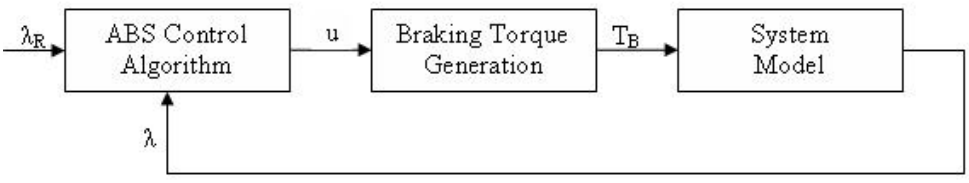

Figure 4.1. Schematic of ABS control

4.1. Mathematical Model

In this study, SMC is used to track reference wheel slip. The main components of this controller are a switching function s to define the sliding surface, an equivalent control braking torque $T_{b,eq}$, a discontinuous control braking torque $T_{b,h}$, and a continuous switching function to avoid chattering.

4.1.1. Design of Sliding Surface

As the main control objective is to keep the wheel slip λ at a desired value, it makes most sense to describe the sliding surface in terms of the error between the actual slip and its desired value. By selecting the order of differentiation $n = 1$, the sliding surface can be defined as [33]:

$$\begin{aligned} s &= (\frac{d}{dt} + \delta)^{(n-1)}(\lambda - \lambda_R) \\ &= (\lambda - \lambda_R) \end{aligned} \tag{4.1}$$

The sliding motion occurs when the state (λ, λ_R) reaches the sliding surface (a point in this case) defined by $s = 0$.

4.1.2. Design of Equivalent Control Braking Torque

The control that keeps the system states on the sliding surface is called "equivalent control". The dynamics along the sliding surface is given by

$$\dot{s} = 0 \tag{4.2}$$

Differentiating Equation (4.1) and substituting into (4.2) results in:

$$\dot{\lambda} = \dot{\lambda}_R \tag{4.3}$$

If it is assumed that the reference wheel speed is constant, i.e., $\dot{\lambda}_R = 0$, we have

$$\dot{\lambda} = 0 \tag{4.4}$$

The dynamics of the ABS laboratory setup are presented in Chapter 2. The formula for the wheel slip derived in this chapter is:

$$\lambda = \frac{r_2\omega_2 - r_1\omega_1}{r_2\omega_2} \tag{4.5}$$

Differentiating λ will result in:

$$\begin{aligned} \dot{\lambda} &= \frac{(\dot{\omega}_1 r_1)(\omega_2 r_2) - (\omega_1 r_1)(\dot{\omega}_2 r_2)}{(\omega_2 r_2)^2} \\ &= \frac{1}{\omega_2 r_2}\left[-\dot{\omega}_1 r_1 + \frac{\omega_1 r_1}{\omega_2 r_2}\,\dot{\omega}_2 r_2\right] \end{aligned} \tag{4.6}$$

The vehicle dynamics of the system are presented as

$$J_1\dot{\omega}_1 = F_t r_1 - (d_1\omega_1 + M_{10} + T_B) \tag{4.7}$$

$$J_2\dot{\omega}_2 = -(F_t r_2 + d_2\omega_2 + M_{20}) \tag{4.8}$$

Describing the vehicle dynamics in terms of $\dot{\omega}_1$ and $\dot{\omega}_2$ gives

$$\dot{\omega}_1 = \frac{1}{J_1}(F_t r_1 - d_1\omega_1 - M_{10} - T_B) \tag{4.9}$$

$$\dot{\omega}_2 = -\frac{1}{J_2}(F_t r_2 + d_2\omega_2 + M_{20}) \tag{4.10}$$

Substituting Equations (4.9) and (4.10) into the Equation (4.6) gives

$$\begin{aligned}\dot{\lambda} &= \frac{1}{\omega_2 r_2}\left[-\left(\frac{r_1}{J_1}\left(F_t r_1 - d_1\omega_1 - M_{10} - T_B\right)\right) + \frac{\omega_1 r_1}{\omega_2 r_2}\left(-\frac{r_2}{J_2}(F_t r_2 + d_2\omega_2 + M_{20})\right)\right] \\ &= \frac{r_1}{\omega_2 r_2 J_1}\left(-F_t r_1 + d_1\omega_1 + M_{10} + T_B\right) - \frac{\omega_1 r_1}{\omega_2^2 r_2 J_2}\left(F_t r_2 + d_2\omega_2 + M_{20}\right) \end{aligned} \tag{4.11}$$

Referring to Equation (4.4), $\dot{\lambda}$ stated in Equation(4.11) should be zero.

$$0 = \frac{r_1}{\omega_2 r_2 J_1}\, T_{B,eq} + \frac{r_1}{\omega_2 r_2 J_1}\left(-F_t r_1 + d_1\omega_1 + M_{10}\right) - \frac{\omega_1 r_1}{\omega_2^2 r_2 J_2}\left(F_t r_2 + d_2\omega_2 + M_{20}\right) \tag{4.12}$$

Solving the Equation (4.12), the equivalent control braking torque can be found as:

$$T_{B,eq} = (F_t r_1 - d_1\omega_1 - M_{10}) + \frac{\omega_1 J_1}{\omega_2 J_2}\left(F_t r_2 + d_2\omega_2 + M_{20}\right) \tag{4.13}$$

Since we can not measure the force F_t directly, it is replaced with the approximation $\widehat{F}_t$. Then $\widehat{T}_{B,eq}$ becomes

$$\widehat{T}_{B,eq} = (\widehat{F}_t r_1 - d_1\omega_1 - M_{10}) + \frac{\omega_1 J_1}{\omega_2 J_2}\left(\widehat{F}_t r_2 + d_2\omega_2 + M_{20}\right) \tag{4.14}$$

4.1.3. Design of Discontinuous Control Braking Torque

If the system state (λ, λ_R) is not on the sliding surface, an additional control term called "discontinuous control braking torque" $T_{b,h}$, should be added to the overall

braking torque control signal. When the system state is on the sliding surface, the discontinuous control has no effect. The discontinuous control braking torque $T_{b,h}$, is determined by the following reaching condition where η is a strictly positive design parameter.

$$s\dot{s} \leq -\eta|s| \tag{4.15}$$

Using Equations (4.2) and (4.4), Equation (4.14) can be rewritten as follows:

$$s\dot{\lambda} \leq -\eta|s| \tag{4.16}$$

The overall braking torque control is assumed to have the form:

$$T_B = \widehat{T}_{B,eq} - T_{B,h}sgn(s) \tag{4.17}$$

Recall that $sgn(s)$ is defined as:

$$sgn(s) = \frac{|s|}{s} \tag{4.18}$$

Substituting Equation (4.11) into Equation (4.16) and using the definition of T_B given in Equation (4.17) result in the following equation:

$$-\frac{sr_1(\omega_2 r_1 J_2 + \omega_1 r_2 J_1)}{\omega_2^2 r_2 J_1 J_2}\,(F_t - \widehat{F}_t) - \frac{r_1 T_{B,h}}{\omega_2 r_2 J_1}|s| \leq \eta|s| \tag{4.19}$$

To ensure Lyapunov stability regardless of η, $T_{B,h}$ is chosen as:

$$T_{B,h} = \frac{\omega_2 r_2 J_1}{r_1}(F + \eta) \tag{4.20}$$

Combining Equations (4.19) and (4.20) gives:

$$-\frac{s r_1(\omega_2 r_1 J_2 + \omega_1 r_2 J_1)}{\omega_2^2 r_2 J_1 J_2}\ (F_t - \widehat{F}_t) \leq F|s| \tag{4.21}$$

$$\frac{r_1(\omega_2 r_1 J_2 + \omega_1 r_2 J_1)}{\omega_2^2 r_2 J_1 J_2}\ |F_t - \widehat{F}_t|_{max}|s| \leq F|s| \tag{4.22}$$

The function F has to be designed to ensure that the reaching condition stated in Equation (4.15) will be satisfied.

$$\frac{r_1(\omega_2 r_1 J_2 + \omega_1 r_2 J_1)}{\omega_2^2 r_2 J_1 J_2}\ |F_t - \widehat{F}_t|_{max} \leq F \tag{4.23}$$

where $|F_t - \widehat{F}_t|_{max}$ is a constant corresponding to the maximum value of the estimation error.

Consequently, the overall braking torque control, T_B, has the form:

$$\begin{aligned} T_B \ &= \ (\widehat{F}_t r_1 - d_1\omega_1 - M_{10}) + \frac{\omega_1 J_1}{\omega_2 J_2}\ (\widehat{F}_t r_2 + d_2\omega_2 + M_{20}) \\ &\quad -\frac{\omega_2 r_2 J_1}{r_1}\left(\frac{r_1(\omega_2 r_1 J_2 + \omega_1 r_2 J_1)}{\omega_2^2 r_2 J_1 J_2}\ |F_t - \widehat{F}_t|_{max} + \eta\right) sgn(s) \end{aligned} \tag{4.24}$$

4.1.4. Design of Continuous Switching Control

The discontinuous switching function $sgn(s)$ in braking torque control specified in Equation (4.22) may give rise to the chattering phenomenon. As mentioned earlier, chattering is highly undesirable as it leads to a high number of oscillations of the system trajectory around the sliding surface and excessive load to the actuators can occur [32]. Ideally, a control strategy is required to ensure that the system dynamic is close to sliding surface $s(t)$.In this thesis, continuous switching $\frac{s}{|s|+\delta}$, where $\delta \geq 0$, is used instead of the discontinuous switching $sgn(s)$ to reduce chattering. Hence, rewriting the overall braking torque with the continuous switching yields

$$T_B = (F_t r_1 - d_1\omega_1 - M_{10}) + \frac{\omega_1 J_1}{\omega_2 J_2}\,(F_t r_2 + d_2\omega_2 + M_{20}) - \frac{\omega_2 r_2 J_1}{r_1}\,\eta\frac{s}{|s|+\delta} \tag{4.25}$$

Using braking torque control, the wheel slip will be regulated at the desired value to satisfy maximum road adhesion coefficient.

4.2. Simulation Results

Simulations are powerful tools to have a general understanding on the behavior of systems for different cases and conditions. In this thesis, to investigate the performance of the proposed controller, Simulink extension of MATLAB is used. To be able to perform simulations, first a block diagram of the system based on its mathematical equations should be created. Figure 4.2 shows the block diagram of the ABS system are shown.

The controller is designed inside the block named *SMC*. The interior of *SMC* is shown in Figure 4.3. as can be seen the controller consist of three subsystems. These are *Equivalent Control*, *Discontinuous Control*, and *Generation of control input u*.

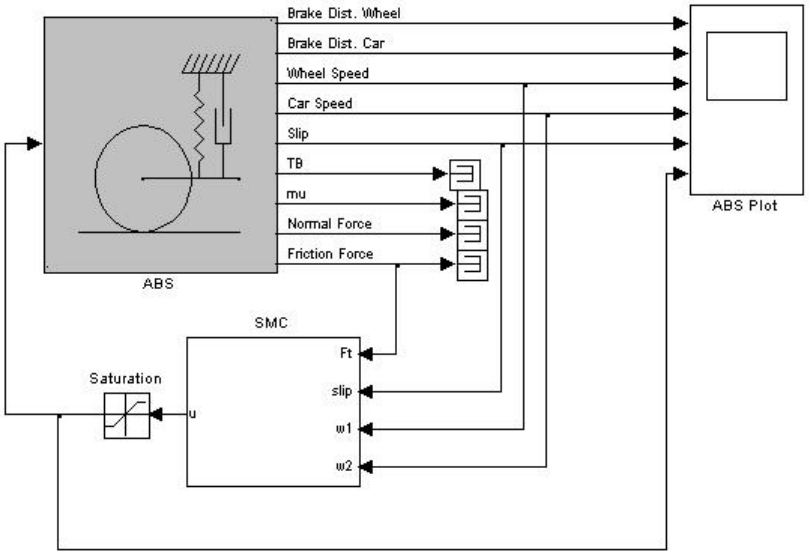

Figure 4.2. Block diagram of ABS control system

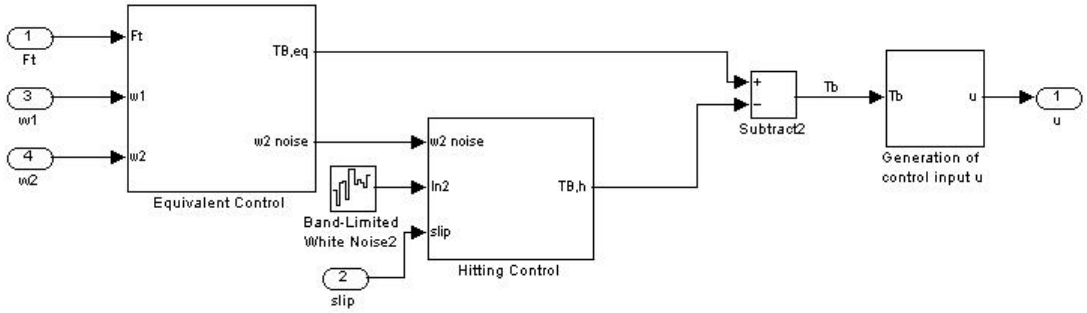

Figure 4.3. Inside of the SMC block of Figure 4.2

The sliding mode control designed in this thesis consists of two parts. These are equivalent control and discontinuous control. The mathematical expressions for both of the controls was derived in the previous section. Using the mathematical expressions, the following subsystems are designed. The other subsystem of *SMC* generates the control input u, which is the input variable for the plant in simulations, based on the value of braking torque and its derivative.

Once the block diagram of the designed controller for ABS setup is complete, simulations can be performed using it. In simulations, it is assumed that the vehicle is braking on a straight line. The initial velocity of the vehicle is set to $V = 70km/h$. The reference wheel slip is first taken to be constant ($\lambda = 0.2$), and then it is considered as a

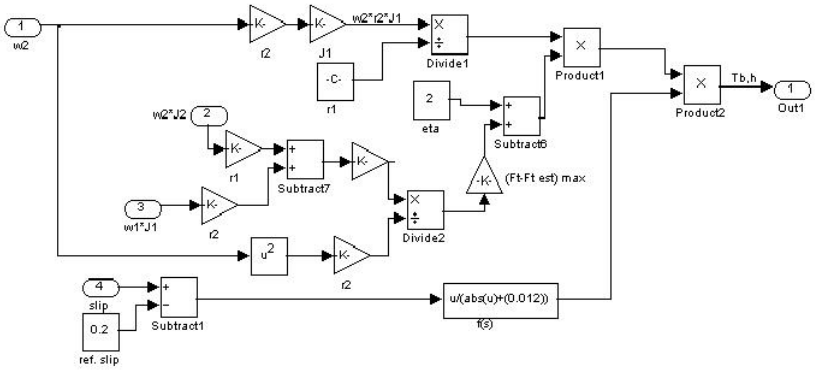

Figure 4.4. Subsystem for discontinuous control

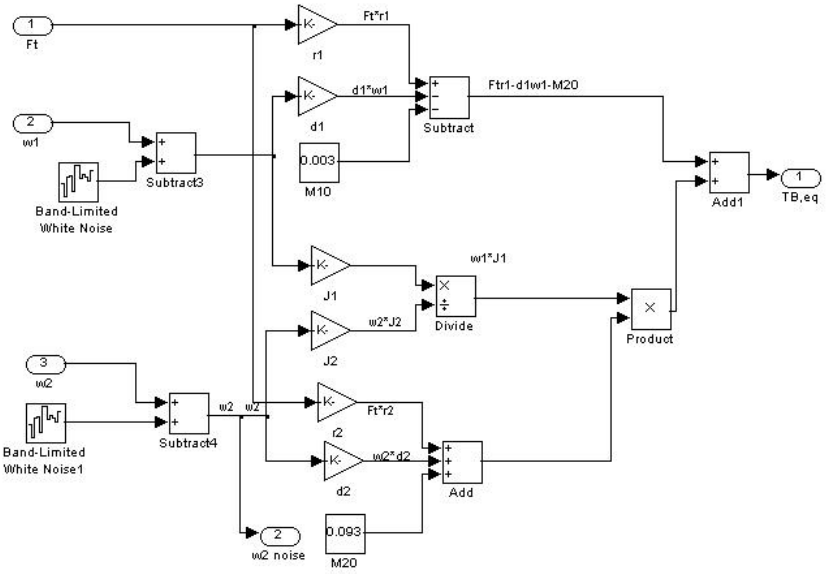

Figure 4.5. Subsystem for equivalent control

function of vehicle velocity. All tests are run for a 1ms sampling period. The numerical values of SMC design parameters η and δ are selected as 2 and 0.01, respectively.

4.2.1. Constant Reference Wheel Slip

In literature, it is common practice to set the reference value of wheel slip to a constant value. In this study, SMC will maintain the wheel slip at $\lambda_R = 0.2$. Regarding the fact that in real life almost every system is subjected to disturbances, band-limited white noise is added to the system at slip and velocity measurements to obtain more realistic results. The controller is expected to keep the noise included system states close to the sliding surface. The numerical value of noise power for slip measurement is

selected 10^{-5}. The noise power for speed measurements is 0.2. Figures 4.6-4.8 illustrate system responses of SMC. As expected, the controller does not possess any steady state errors. SMC is capable of stopping the car in approximately 1.4 seconds. The braking distance is around 10.8 meters.

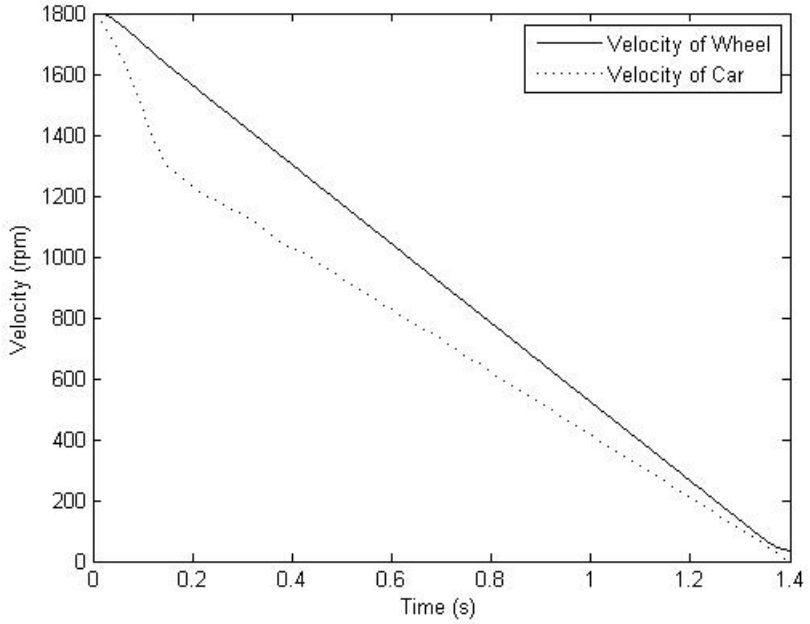

Figure 4.6. Wheel and vehicle velocities for constant reference

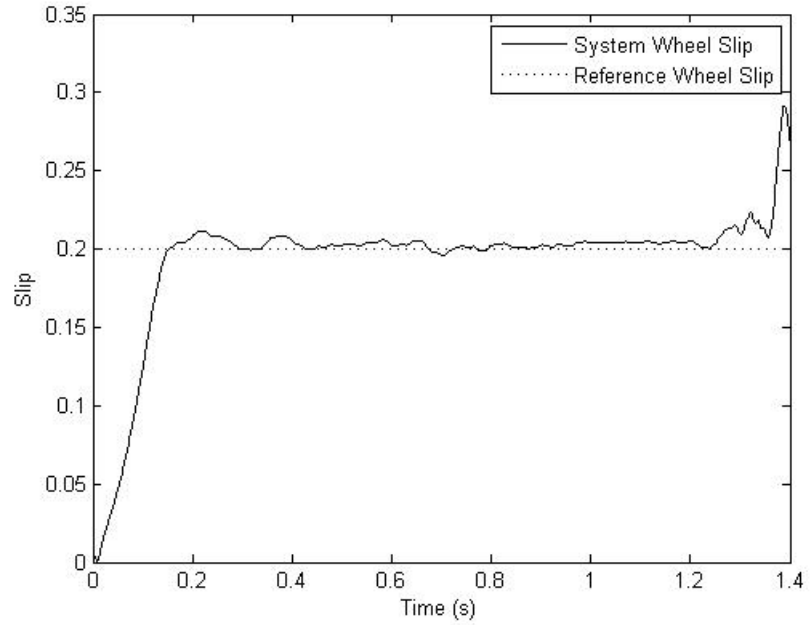

Figure 4.7. Wheel slip of SMC for constant reference

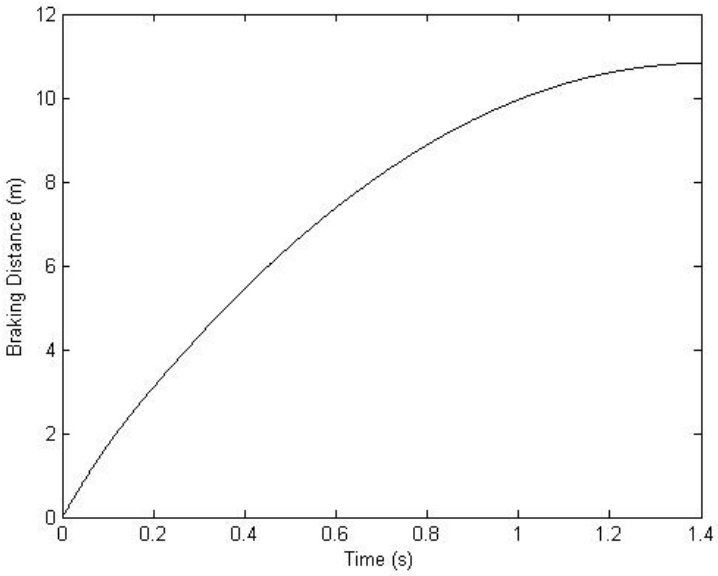

Figure 4.8. Braking distance of SMC for constant reference

4.2.2. Velocity Dependent Reference Wheel Slip

In this part, it is assumed that the road adhesion coefficient does not only depend on wheel slip, on the contrary, it is a nonlinear function of vehicle velocity and wheel slip. To find the optimum value of wheel slip for the changing speed of the vehicle, the pseudo-static curves of Equation (2.10) are plotted. It is assumed that the velocity of the car can vary within the range $0m/s$ and $30m/s$. From the graphs, the maximum wheel slip is determined for each velocity value of the vehicle. To calculate the road adhesion coefficient corresponding to a wheel slip value, the formula expressed in Equation (2.9) has been used. A look up table is constructed to relate car speed to the road adhesion coefficient and reference wheel slip. The system responses of SMC for variable reference wheel slip have been presented in Figures 4.9 to 4.11.

Regarding the simulation results, it can be inferred that SMC can track the reference wheel slip precisely. Similar to the previous case, there is no steady state error in SMC. The stopping time of the car is approximately 1.4 seconds, which is the same value as in the previous case. The difference in braking distance is more obvious. It is reduced to 9.6 meters, which corresponds to a 11 per cent improvement.

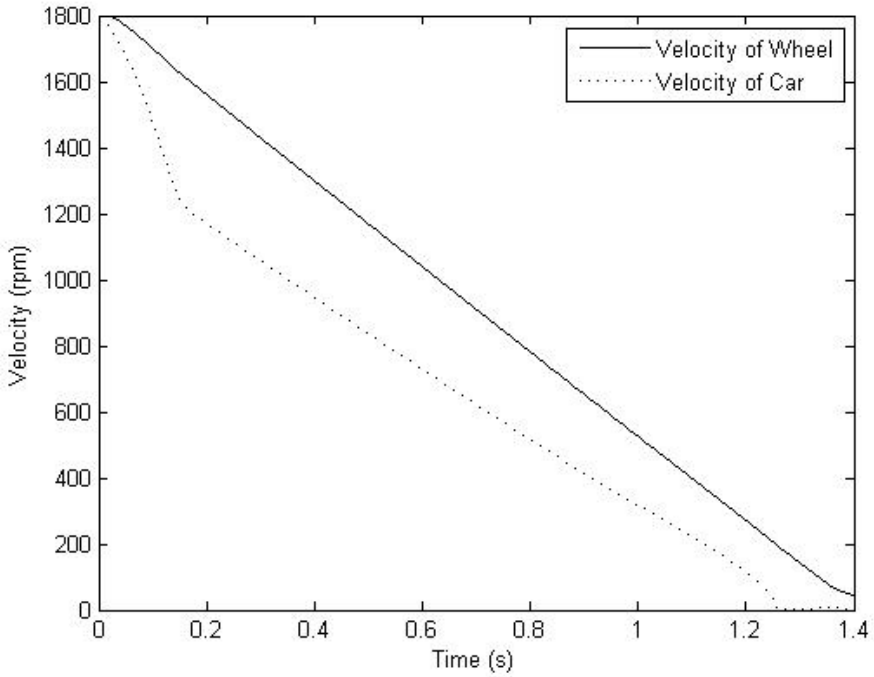

Figure 4.9. Wheel and vehicle velocities for velocity dependent reference

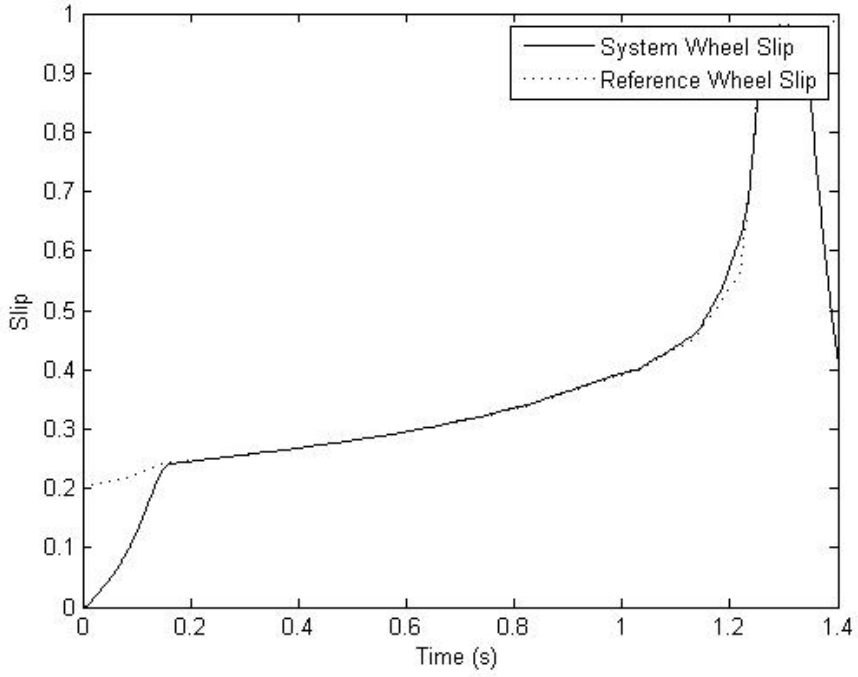

Figure 4.10. Wheel slip of SMC for velocity dependent reference

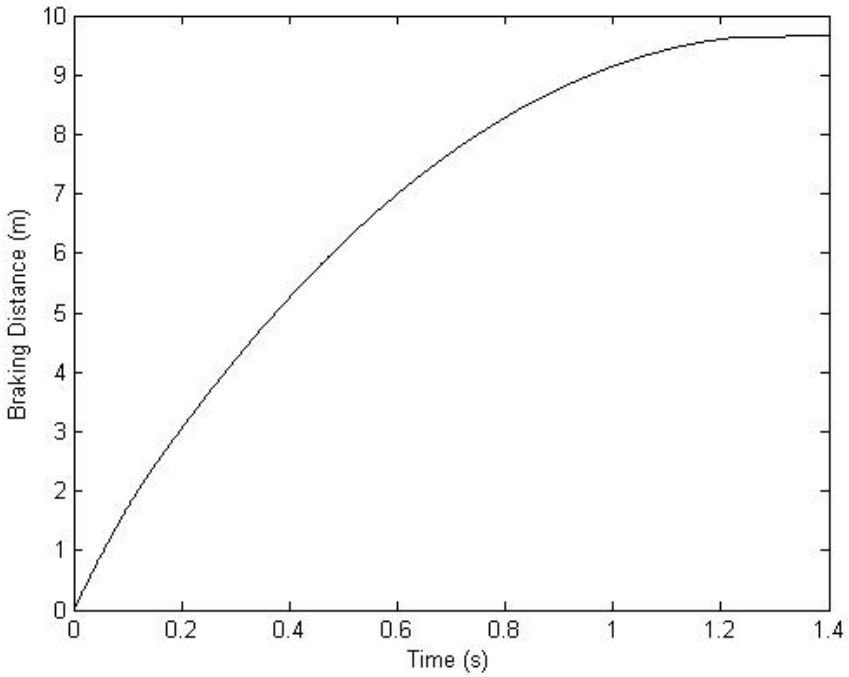

Figure 4.11. Braking distance of SMC for velocity dependent reference

4.3. Experimental Results

For the experiments, the ABS setup of Inteco Ltd. has been used. To imitate the behavior of the vehicle during braking on a dry and straight road, the wheel is accelerated until the velocity of the wheel reaches $70km/h$. Once it reaches the velocity limit, the braking operation is started. There is another velocity threshold which states the minimum velocity level for applying ABS control algorithms. Under this minimum value of the velocity, the system becomes unstable if the ABS algorithm is applied. Under such a circumstance, the maximum braking torque should be applied to the wheels without considering the target value of slip. In this study, the lower velocity threshold value has been chosen $V = 5km/h$.

In the previous section, it was observed that the proposed controller works adequately for the ABS system. In this section, the real time response of the controller will be compared with simulation results. In the experiments, also two different approaches will be followed to determine the reference value of wheel slip. In the first approach, the reference wheel slip is constant throughout the braking process. Next,

it is defined as a velocity dependent variable. In experiments, there is no need to add external disturbance to the measurements, as the measurements are already noisy. For experiments, a fixed-step type of solver should be used. The step size is set to $1ms$. For all the experiments, SMC design parameters are as follows: $\eta = 2$ and $\delta = 0.01$.

4.3.1. Constant Reference Wheel Slip

The results of the experiment for constant reference wheel slip have been presented in the figures below. It can be concluded that the performance of the proposed controller is acceptable, as even in the presence of disturbances from both the interior and exterior, SMC still can track the reference wheel slip satisfactorily.Although in the simulation model the vehicle stops in 1.4 seconds, in real time experiments only 0.6 seconds have been needed to stop the vehicle. The difference in stopping times may result from the imperfections in the modelling. The settling time is approximately 0.05 seconds.

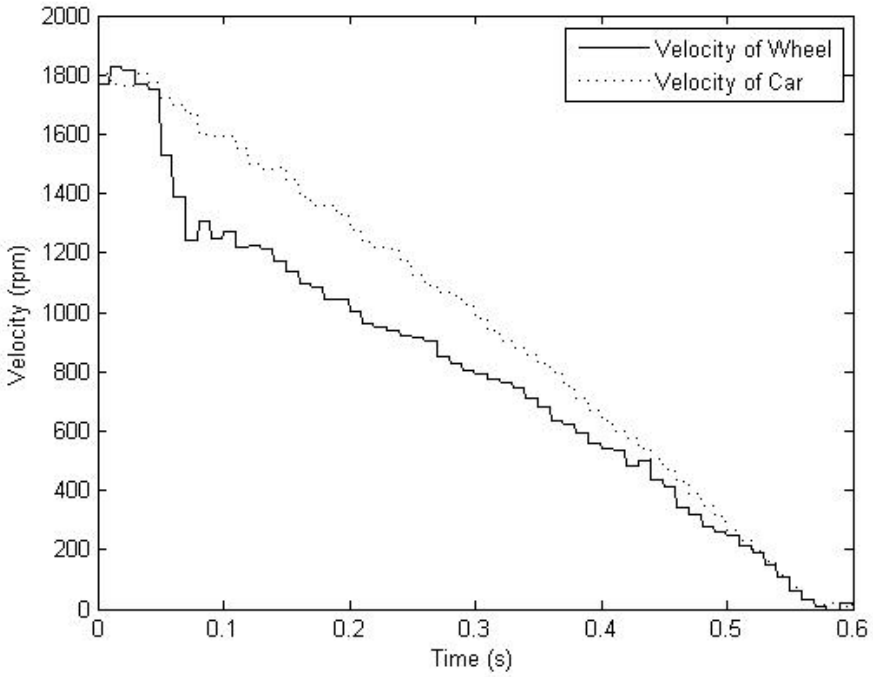

Figure 4.12. Experimental results of wheel and vehicle velocities for constant reference

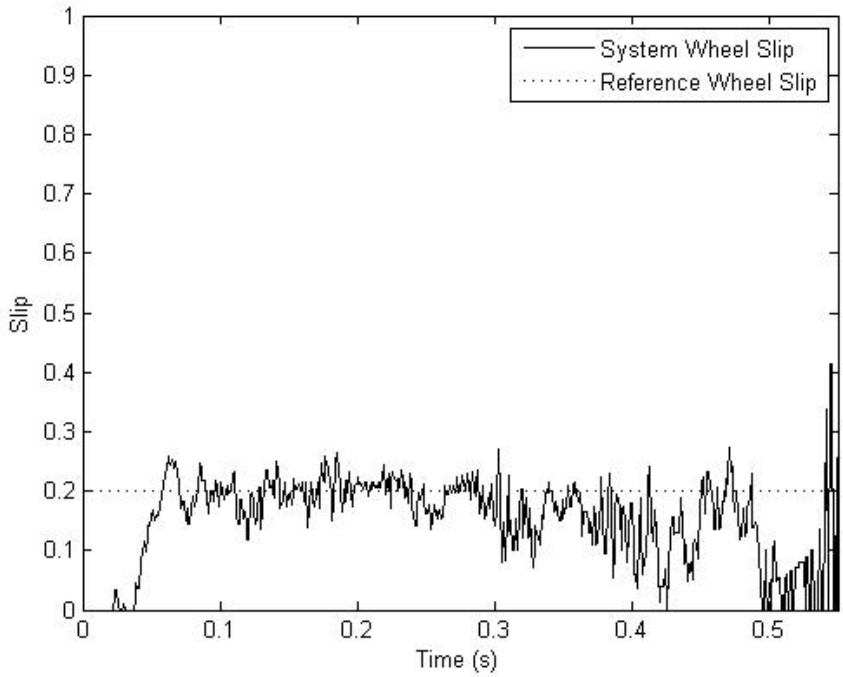

Figure 4.13. Experimental results of wheel slip for constant reference

4.3.2. Velocity Dependent Reference Wheel Slip

Employing the velocity dependent approach to determine the optimal value of wheel slip will result in the Figures 4.14 and 4.15. Referring to these figures, the performance of SMC is mainly satisfactory. Although there are some deviations from the reference value, the wheel slip of the system stays close to the reference value. When the experimental results are compared with the simulation results, it can be observed that they are consistent and similar. The differences between the results may stem from several reasons including the incomplete model of the system and nonlinearities involved in real life applications.

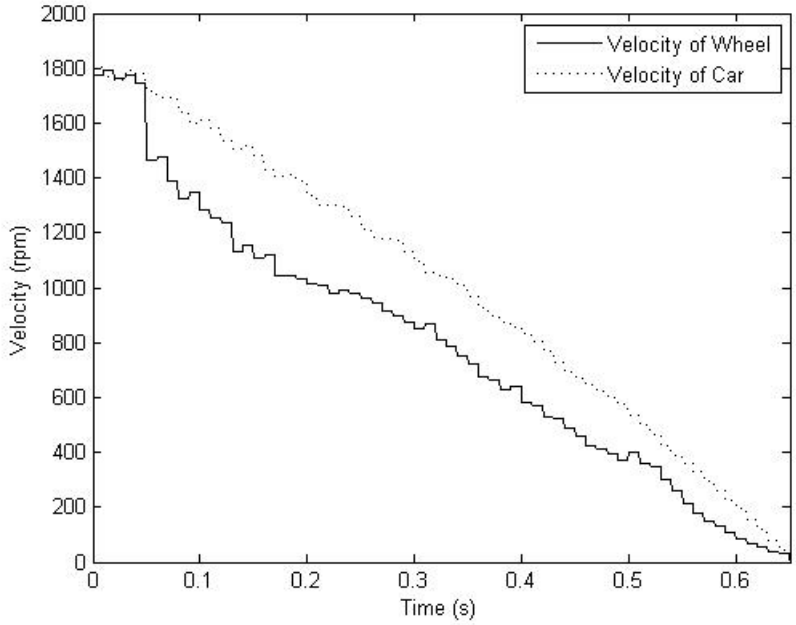

Figure 4.14. Experimental results of wheel and vehicle velocities for velocity dependent reference

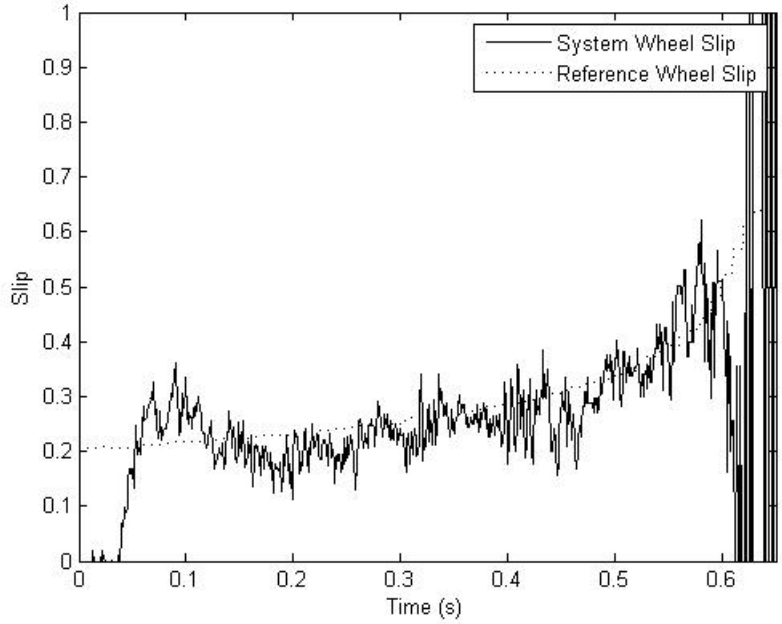

Figure 4.15. Experimental results of wheel slip for velocity dependent reference

4.4. Discussions

In this chapter, a sliding mode controller has been designed using the system equations presented in Chapter 2. The selection of SMC relies on the fact that ro-

bust control algorithms should be applied to the system of interest to deal with the uncertainties and nonlinearities. The design process based on the Lyapunov stability approach consists of two parts: The design of equivalent control and the design of discontinuous (or striking) control.

In the second part of the chapter, the simulation model and simulation results of SMC have been derived and discussed. Due to the noise added to the system to imitate real life conditions, SMC can not exactly move along the sliding surface; however its performance is acceptable, as the system states stay in the neighborhood of $s(t)$.

The designed simulation model has been implemented on the real-time system. The results of the experiments are similar to the simulation results although there are some differences that can be attributed to internal and external disturbances applying on the real time system. In the forthcoming chapters, the design of SMC will be developed by coupling a grey predictor to it.

5. GREY SYSTEM THEORY AND CONTROLLER DESIGN

Grey System Theory was first proposed in 1980 by J. L. Deng, who is a professor in Hua Chung Science and Engineering University. This was a new theory and method which can be applied to solve numerous problems with few or incomplete data, as it possessed the ability to make full use of limited data to predict the future values of the system parameters. Two years later, in 1982, Professor Deng published the first research paper titled "Control Problems of Grey Systems" in the international journal "Systems and Control Letters" [35].

Although Grey System Theory was a fairly new interdisciplinary scientific area, it had a profound impact on the researchers and practitioners during the last two decades, and has been widely used in the analysis, prediction, modeling, decision-making and control of various systems [36]. A pioneering example of the application of the grey prediction controller to regulate an industrial process of an unknown system model was achieved by Cheng in 1986 [37]. Encouraged by the successful results of this study, grey models have been implemented in a variety of fields including agriculture [38], power systems [39], geology [40] and control systems [41].

The main advantage of grey prediction is that it requires only limited data to develop the grey model compared to the conventional controllers which need samples of reasonable size and good distribution of the data to develop an appropriate model. Because of this ability, the grey predictor is an excellent candidate to be applied to real time control systems. Although most of the researchers of this theory are from the Far Eastern countries, in 1989 the first academic magazine entitled "The Journal of Grey System" was published in England with the aim to publish articles covering both theoretical and applied aspects of the Grey System Theory and its application.

In 1994, Huang designed a grey predictor coupled to a fuzzy controller to control an inverted pendulum, which is a fundamental control problem in the literature [42]. Two years later, Huang offered a genetic-based fuzzy grey prediction model to compensate the output of grey system [43]. In 1998, Wong designed a switch grey prediction fuzzy controller to determine the appropriate forecasting step size for a grey predictor [44]. In 2002, Lin presented a technique to adjust the inner parameter values of the grey model, which plays a major role in the improvement of accuracy of the grey predictor [45].

A major milestone in the history of Grey System Theory was the establishment of the Chinese Grey System Association (CGSA) in 1996 with the mission to promote this theory among researchers by organizing conferences every year. Furthermore, the courses and workshops offered in China, Taiwan, Japan, Singapore, Hong Kong, USA, Canada, England, and Australia on grey systems help to have a better understanding of how important and popular the Grey System Theory has become. Recently, Grey System Theory has been listed in many international conferences as a special topic, and numerous journals on this topic have been published. Figure 5.1 shows the number of papers published in the last twenty years. Based on this figure, it can be concluded that there is increasing tendency to the topic.

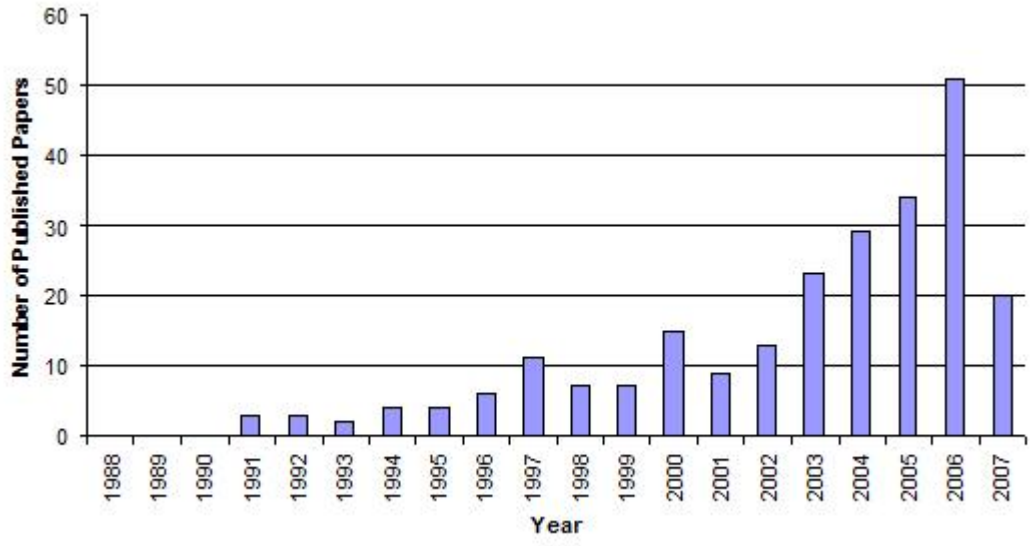

Figure 5.1. Number of published papers on grey systems between January 1988 and June 2007 (Source: Web of Science)

5.1. Fundamental Concepts of Grey Systems

It is a convenient method to describe a system with a color based on the clarity of information about that system. A system can be described as "black" if the internal relations between system parameters or mathematical equations describing the dynamics of the system are totally unknown. Such systems are also referred to as "black box", as only the inputs and outputs of the system are observable, but there is no information about the internal structure which relates system inputs to the outputs. On the contrary, if the structure and dynamics of the system are totally available for inspection, it can be named as a "white" system. In a similar manner, "grey" will refer to information that is partially known and partially unknown. In real life, almost every system can be called a grey system because there is always some uncertainty involved due to the noise from both inside and outside of the system [46].

In daily social, economic and scientific activities, situations of incomplete information are very common. For instance, in some studies related with agriculture, although the information about the land that will be planted, the quality of seeds, fertilizers, etc., is completely known, still it is very challenging to estimate the annual production quantity due to various unknown and vague parameters including weather conditions, the natural environment, and labor quality [47]. Similarly, the data collected from a motor control system usually involves some uncertain characteristics because of the time-varying parameters of the system and difficulties arising in the measurements [48].

Incomplete information is the fundamental meaning of being "grey". Liu states four possibilities for incomplete information of systems as follows [47]:

- The information of parameters or system elements is incomplete.
- The structural information is incomplete
- The boundary information is incomplete.
- The behavior information motion is incomplete.

For different circumstances, the meaning of "black", "grey", and "white" can

vary. These have been summarized in Table 5.1.

Table 5.1. The meaning of black, grey, and white

	Black	**Grey**	**White**
Information	unknown	incomplete	known
Appearance	dark	grey	bright
Process	new	replace old with new	old
Property	chaos	complexity	order
Methodology	negative	transition	positive
Attitude	indulgence	tolerance	surety
Conclusion	no result	multiple solution	unique solution

Grey System Theory and grey controllers offer great performance in situations with a small sample size where any prior experience about the system or a special distribution of sample data is not available. The behavioral characteristics of the system of interest are established by using a sequence of definite white numbers. However, the complexity and disordered structure of the data may mislead the controller. To deal with this problem, some sequence operators are used in the grey controllers to smooth the data, which will enable derivation of the characteristics of the system easily.

5.2. Grey System Modeling

5.2.1. Grey Numbers

The entire theory of grey systems lies on the foundation of grey numbers and their operations, grey matrices and grey equations, as each grey system is described in terms of these terms. A grey number, which is the elementary "atoms" of a grey system, is a number whose value is not exactly known. Instead, the interval or range within which the number lies is known [47]. A grey number, which is denoted by the sign $\otimes$, can be bounded by an upper limit, a lower limit, or both. For instance, a grey

number with a lower limit but no upper limit can be presented as:

$$\otimes \in [\underline{a}, \infty) \qquad or \qquad \otimes (\underline{a})$$

where $\underline{a}$ is a fixed number that represents the lower limit of the grey number . The term $[\underline{a}, \infty)$ is called value field of the grey number the $\otimes$, or briefly a grey field.

5.2.2. Generations of Grey Sequence

In Grey System Theory, one of the main tasks is to determine realistic governing laws from the data available. This process is called *generations of grey sequence* [47]. It is believed that even though the available data might be complicated and chaotic, there should always be some governing rules which describe the behavior of the system as a whole.

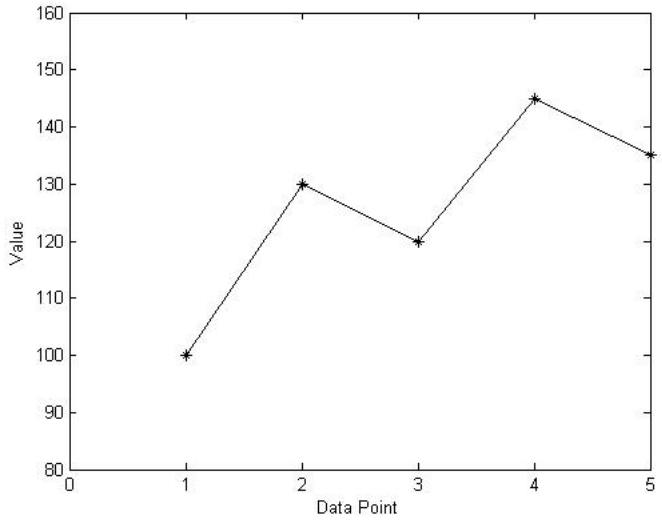

Figure 5.2. Graphical representation of the original data set

In Grey System Theory, it is argued that reducing the randomness in the grey sequence through some generations will help to find out the regularities in the system. "Accumulating Generation" is the most common method used to uncover these regularities. Let's assume that the following sequence is given:

$$X^{(0)} = (100, 130, 120, 145, 135)$$

Obviously the given sequence does not have any clear regularity. Hence, it is almost impossible to draw a conclusion about the system behavior based on this data. However, if accumulating generation is applied to the original sequence $X^{(0)}$, the resulting sequence $X^{(1)}$ will have a clear growing tendency.

$$X^{(1)} = (100, 230, 350, 495, 630)$$

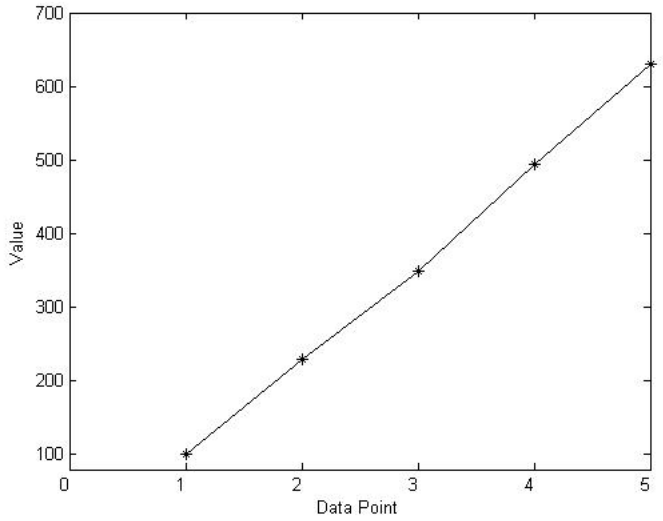

Figure 5.3. Graphical representation of the accumulated data set

5.2.2.1. Accumulating Generating Operation (AGO). The accumulating generating operation (AGO) is a method that is commonly used to whiten a grey process. Through accumulation, the development and tendency of a grey sequence can be seen, which allows the uncovering of special characteristics or laws hidden in the chaotic raw data [47].

Consider that $X^{(0)}$ is a nonnegative sequence of raw data and D is a sequence operator:

$$X^{(0)} = \left(x^{(0)}(1), x^{(0)}(2), ..., x^{(0)}(n)\right) \tag{5.1}$$

and

$$X^{(0)}D = \left(x^{(0)}(1)d, x^{(0)}(2)d, ..., x^{(0)}(n)d\right) \tag{5.2}$$

where

$$x^{(0)}(k)d = \sum_{i=1}^{k} x^{(0)}(i) \qquad for \;\; k = 1, 2, ..., n \tag{5.3}$$

D is called *first order accumulating generator* of $X^{(0)}$ and it is denoted as $1-AGO$. The rth-order operator D^r can be obtained by applying D operation r times, which will be denoted as $r - AGO$.

$$X^{(0)}D = X^{(1)} = \left(x^{(1)}(1), x^{(1)}(2), ..., x^{(1)}(n)\right) \tag{5.4}$$

and

$$X^{(0)}D^r = X^{(r)} = \left(x^{(r)}(1), x^{(r)}(2), ..., x^{(r)}(n)\right) \tag{5.5}$$

where

$$x^{(r)}(k)d = \sum_{i=1}^{k} x^{(r-1)}(i) \qquad for \;\; k = 1, 2, ..., n \tag{5.6}$$

5.2.2.2. Inverse Accumulating Generating Operation (IAGO). As the name implies, "inverse accumulating generation operation" (IAGO) is the inverse operation of accumulating generating operation. It is used for the recovery of the original data often used when there is a need for additional information [47].

Assume that $X^{(1)}$ is a nonnegative sequence of raw data, and $\overline{D}$ is a sequence

operator. Then

$$X^{(1)} = \left(x^{(1)}(1), x^{(1)}(2), ..., x^{(1)}(n)\right) \tag{5.7}$$

and

$$X^{(1)}\overline{D} = \left(x^{(1)}(1)\overline{d}, x^{(1)}(2)\overline{d}, ..., x^{(1)}(n)\overline{d}\right) \tag{5.8}$$

where

$$x^{(1)}(k)\overline{d} = x^{(1)}(k) - x^{(1)}(k-1) \qquad for \;\; k = 1, 2, ..., n \tag{5.9}$$

$\overline{D}$ is called *first order inverse accumulating generator* of $X^{(1)}$, and it is denoted as $1 - IAGO$. The rth-order operator $\overline{D}^r$ of $X^{(1r)}$ can be obtained by applying $\overline{D}$ operation r times, which will be denoted as $r - IAGO$.

$$X^{(1)}\overline{D} = X^{(0)} = \left(x^{(0)}(1), x^{(0)}(2), ..., x^{(0)}(n)\right) \tag{5.10}$$

and

$$X^{(r)}\overline{D} = X^{(r-1)}\overline{D}^{(r-1)} = \left(x^{(r-1)}(1), x^{(r-1)}(2), ..., x^{(r-1)}(n)\right) \tag{5.11}$$

where

$$x^{(r-1)}(k) = x^{(r)}(k) - x^{(r)}(k-1) \qquad for \;\; k = 1, 2, ..., n \tag{5.12}$$

5.2.3. Grey Differential Equations

Differential equations, which relate the derivative of a function to the function itself as well as the independent variable, are very important because the laws of nature

are most often expressed in terms of them. Once the differential equation of a system is obtained, it is relatively simple to solve the problem. The concept of grey derivatives is introduced to establish a system model similar to differential equations using the sequence of discrete data.

Consider the following differential equation:

$$\frac{dx}{dt} + ax = b \tag{5.13}$$

In this equation, dx/dt stands for the *derivative* of the function x, x is the *background value* of dx/dt, and a and b are *parameters*. Hence, a differential equation consists of three parts: derivative, background value, and parameters. A grey differential equation should also include these three parts.

The following equation is a grey differential equation:

$$x^{(0)}(k) + az^{(1)} = b \tag{5.14}$$

where

$$z^{(1)}(k) = 0.5x^{(1)}(k) + 0.5x^{(1)}(k-1) \tag{5.15}$$

In these equations, $z^{(1)}(k)$ is the background value, the components $x^{(1)}(k)$ and $x^{(1)}(k-1)$ constitute the grey derivative, and a and b are parameters.

5.2.4. GM(1,1) Model

In Grey System Theory, a grey model is described in terms of the order of differential equations and the number of variables. The general form of the representation of a grey model can be stated as $GM(n, m)$ where n is the order of the differential equation that is used to represent the system and m is the number of system variables. Generally, there are a few types of grey models used in the literature. These are:

- *GM(1,1)* This model is generally used for prediction purposes. It represents a first-order derivative, containing one input variable.
- *GM(1,N)* This model can be utilized for multi-variable analyses. It represents a first-order derivative, but containing N input variables.

- *GM(0,N)* This model is also used for prediction purposes. It represents a zero-order derivative, containing N input variables. This model is a static model, as it does not contain derivatives.

Among these models, $GM(1,1)$, which is pronounced as "Grey Model First Order One Variable", is most widely used in the literature for forecasting purposes. In many studies, it was applied to controller design as a predictor [49]. The ability of prediction stems from the time varying coefficients. First, the $GM(1,1)$ model is constructed based on the original raw data. To do this, at least four data points are required. Then when new data become available, the model is renewed.

To establish the $GM(1,1)$ model, three fundamental operations are required. These are the accumulating generation operation (AGO), the mean operation, and the inverse accumulating generation operation (IAGO). AGO is employed to smooth the randomness in the raw data. Mean operation is used to compute the background value $z^{(1)}(k)$ of the grey differential equation from the components $x^{(1)}(k)$ and $x^{(1)}(k-1)$. Finally, IAGO is applied to find the predictive values corresponding to the original data.

Assume that

$$X^{(0)} = \left(x^{(0)}(1), x^{(0)}(2), ..., x^{(0)}(n)\right) \qquad for \quad n \geq 4 \tag{5.16}$$

where $X^{(0)}$ is a nonnegative sequence and n is the size of the sample data. Applying AGO to the sequence $X^{(0)}$ will result in $X^{(1)}$ which is defined as:

$$X^{(1)} = \left(x^{(1)}(1), x^{(1)}(2), ..., x^{(1)}(n)\right) \qquad for \quad n \geq 4 \tag{5.17}$$

where

$$x^{(1)}(k) = \sum_{i=1}^{k} x^{(0)}(i) \qquad for \quad k = 1, 2, ..., n \tag{5.18}$$

The generated mean sequence $Z^{(1)}$ of $X^{(1)}$ is given as:

$$Z^{(1)} = \left(z^{(1)}(1), z^{(1)}(2), ..., z^{(1)}(n)\right) \tag{5.19}$$

$z^{(1)}(k)$ can be computed by mean operation; i.e. it yields the main value of two adjacent data.

$$z^{(1)}(k) = 0.5x^{(1)}(k) + 0.5x^{(1)}(k-1) \qquad for \quad k = 2, 3, ..., n \tag{5.20}$$

Recall from the previous section that a grey differential equation has the form:

$$x^{(0)}(k) + az^{(1)}(k) = b \tag{5.21}$$

Then the whitening equation can be found as:

$$\frac{dx^{1}(t)}{dt} + ax^{(1)}(t) = b \tag{5.22}$$

If $[a, b]^T$ from the above equation is a sequence of parameters and it can be computed as follows:

$$[a, b]^T = (B^T B)^{-1} B^T Y \tag{5.23}$$

where

$$Y = \left[x^{(0)}(2), x^{(0)}(3), ..., x^{(0)}(2)\right]^T, \tag{5.24}$$

$$B = \begin{bmatrix} -z^{(1)}(2) & 1 \\ -z^{(1)}(3) & 1 \\ \vdots & \vdots \\ -z^{(1)}(n) & 1 \end{bmatrix} \tag{5.25}$$

According to Equation (5.22), the solution of $x^{(1)}(t)$ at time k:

$$x_p^{(1)}(k+1) = \left[x^{(0)}(1) - \frac{b}{a}\right] e^{-ak} + \frac{b}{a} \tag{5.26}$$

To obtain the predicted value of the primitive data at time (k+1), the IAGO is used to establish the following grey model.

$$x_p^{(0)}(k+1) = \left[x^{(0)}(1) - \frac{b}{a}\right] e^{-ak}(1 - e^a) \tag{5.27}$$

and the predicted value of the primitive data at time $(k + H)$:

$$x_p^{(0)}(k+H) = \left[x^{(0)}(1) - \frac{b}{a}\right] e^{-a(k+H-1)}(1 - e^a) \tag{5.28}$$

The parameter $(-a)$ in the GM(1,1) model is called "development coefficient" which reflects the development states of $X_p^{(1)}$ and $X_p^{(0)}$. The parameter b is called "grey action quantity" which reflects changes contained in the data because of being derived from the background values [47].

5.3. Integration of Grey Prediction to SMC

In this thesis, the grey predictor is coupled to a sliding mode controller. This combination is referred to as *Grey Sliding Mode Controller* (GSMC). A grey predictor is employed to anticipate the future outputs of the system using current data available. The grey predictor estimates the forthcoming value of wheel slip and SMC takes the necessary action to maintain wheel slip at the desired value.

Different types of grey models have been presented in the previous section. For this study, the grey model of type $GM(1,1)$ will be utilized. The GM(1,1) type of grey model is most widely used in the literature, pronounced as "Grey Model First Order One Variable". This model is a time series forecasting model. The differential equations of the GM(1,1) model have time-varying coefficients. In other words, the model is renewed as new data become available to the prediction model.

In order to smooth the randomness, the primitive data obtained from the system to form the GM(1,1) is subjected to an operator, named Accumulating Generation Operation (AGO) [50]. The differential equation (i.e. GM(1,1)) thus evolved is solved to obtain the n-step ahead predicted value of the system. Finally, using the predicted value, Inverse Accumulating Generation Operation (IAGO) is applied to find the predicted values of original data. The mathematical operations that are required to establish GM(1,1) were presented in the previous chapter. In this chapter, the integration of grey prediction to the SMC will be the main focus. The performance of a new control scheme called GSMC will be investigated by simulations and experimental studies.

Earlier in this study, the mathematical foundations and governing equations of SMC have been explained. In this section, the coupling of the grey predictor to SMC will be examined.

To integrate grey prediction into the proposed SMC, a new time-varying grey

sliding surface $s(\lambda;t)$ is defined as [51]:

$$s(\lambda,t) = (e + e_p) \tag{5.29}$$

where e is the system error, $e_p = \lambda_R - \lambda_p$ is a value predicted by GM(1,1) model and λ_p is the predicted value of wheel slip. If the Lyapunov candidate function V_L is defined as:

$$V_L = \frac{1}{2}\left(s(\lambda,t)\right)^2 \tag{5.30}$$

then it is guaranteed that the tracking error of GSMC will be less than the one of conventional SMC [51]. The structure of the proposed GSMC has been shown in Figure 6.1.

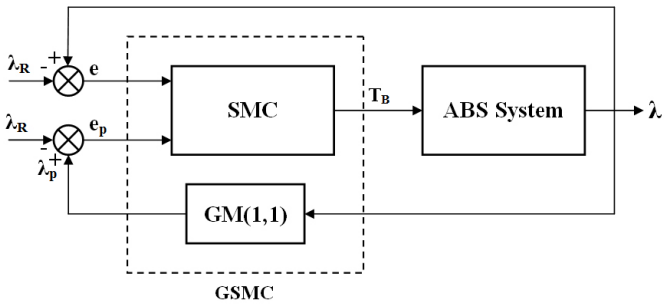

Figure 5.4. Structure of GSMC

5.4. Simulation Results

To investigate he performance of GSMC, numerous computer simulations have been performed. The simulation model of GSMC is similar to the model of SMC. The main difference between them is the addition of the block called *grey predictor*. The wheel slip is the input for this component. The grey predictor estimates the forthcoming values of wheel slip using its current and preceding values. With the information on the wheel slip values beforehand, SMC can control the system more effectively.

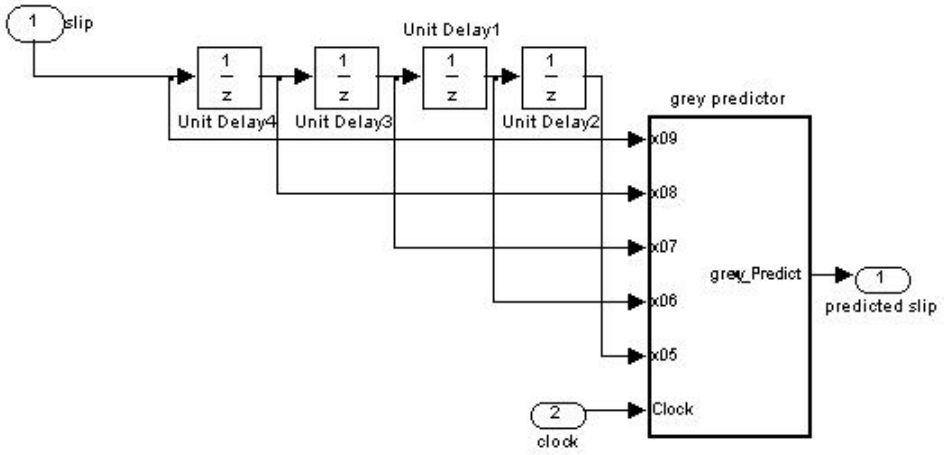

Figure 5.5. Structure of grey predictor

For the simulations of GSMC, two different approaches are applied to determine the reference values of wheel slip. First, it is considered that the reference wheel slip is a constant ($\lambda_R = 0.2$). Next, it is defined as a function of vehicle velocity and a look up table is constructed to relate the reference wheel slip to the velocity of car. In all simulations, it is assumed that the initial velocity of the car is $70km/h$.

5.4.1. Constant Reference Wheel Slip

In the design of GSMC, it is assumed that a SMC with prediction capability can perform better than a conventional SMC. To test this idea, in this section, the simulation results of SMC and GSMC are presented together. From Figure 6.3 to Figure 6.5, the simulation results of GSMC and SMC for constant reference wheel slip have been presented. The step size of GSMC is considered as a constant value, which is 80. In order to obtain more real-like results, band-limited white noise has been added to the system at slip and speed measurements. The numerical values of the design parameters η and δ are selected as 1.2 and 0.2, respectively. The numerical value of the noise power added to the slip measurement is 10^{-5}, whereas the noise power for speed measuremnents is 0.2. Although both controllers do not have steady state errors due to inserted white noise, GSMC exhibits a slightly better performance when compared to conventional SMC. Both controllers are capable of stopping the car in approximately 1.4 seconds and they possess similar braking distances.

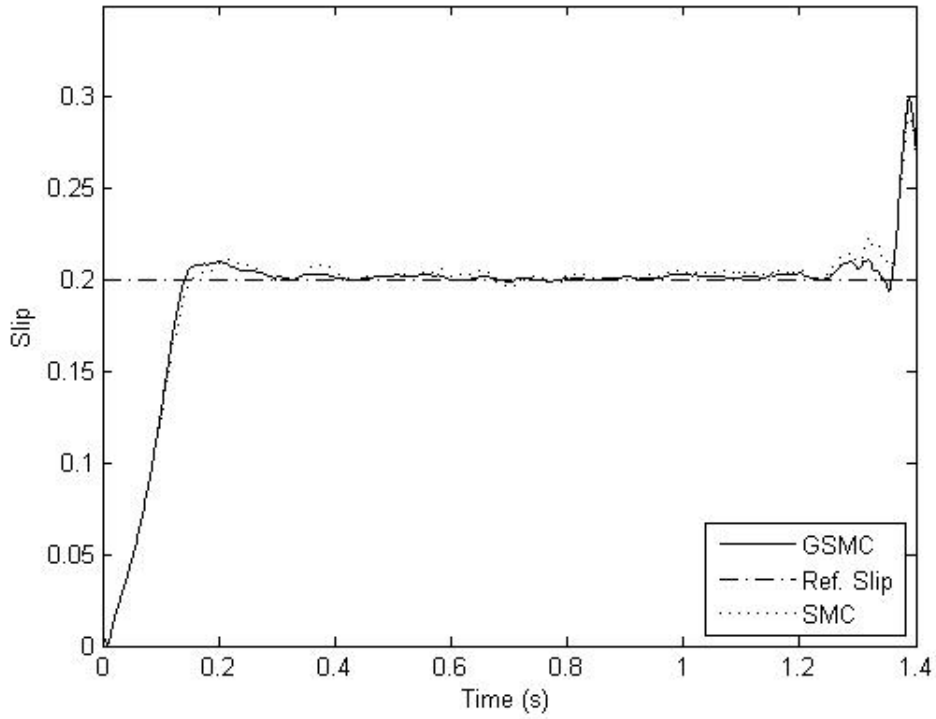

Figure 5.6. Wheel slip of SMC and GSMC for a constant reference

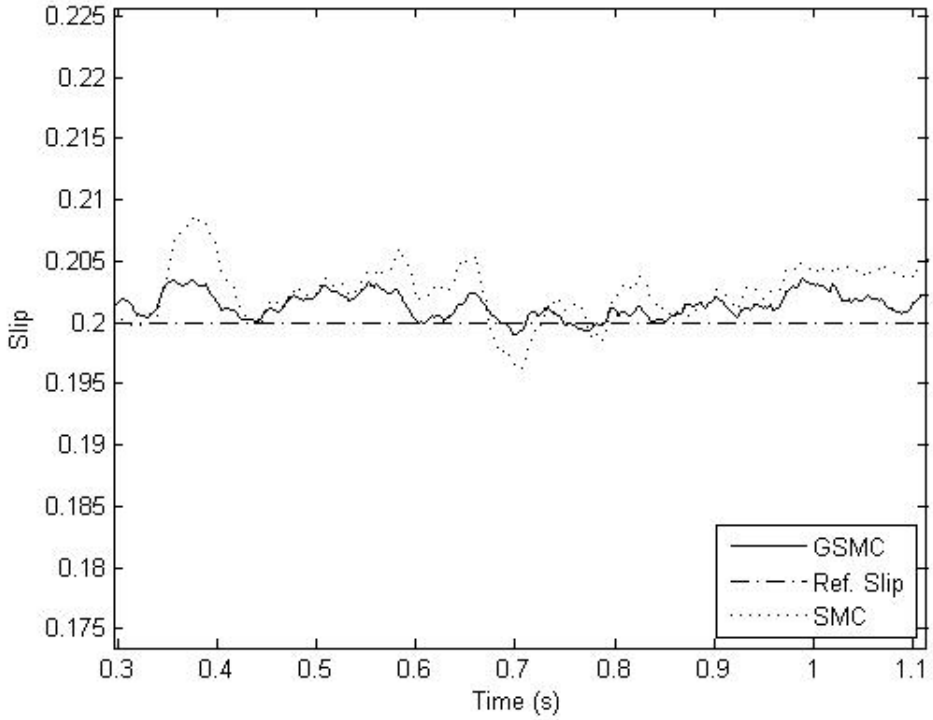

Figure 5.7. Zoomed view of Figure 5.6

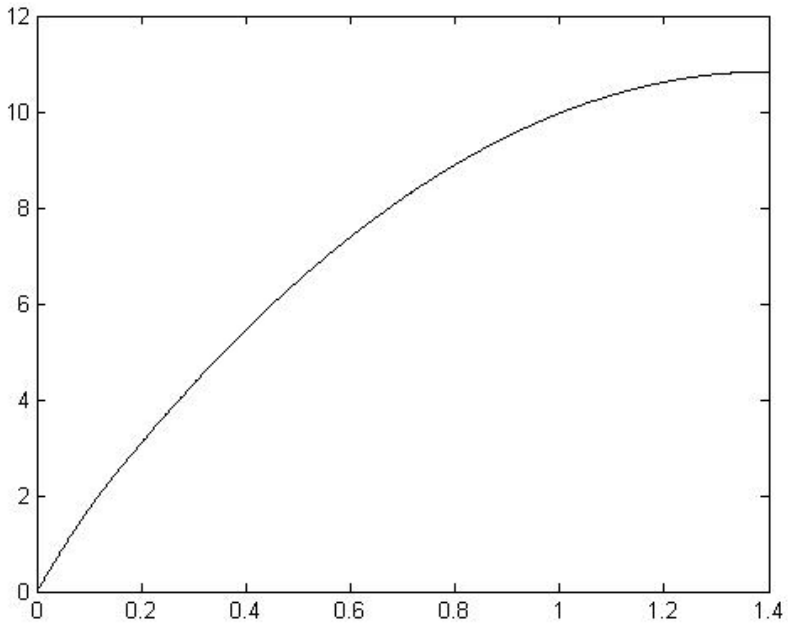

Figure 5.8. Braking distance of SMC and GSMC for a constant reference

5.4.2. Velocity Dependent Reference Wheel Slip

The figures presented below show simulation results of GSMC for velocity dependent reference wheel slip determined using the formula presented in Equation (2.10). Regarding the simulation results, it can be inferred that GSMC can track the reference wheel slip satisfactorily. In this simulation, band limited white noise has not been added to the system. Hence, perfect traction of the reference value has been achieved. Similar to the previous case, the braking distance, 9.7 meters, is shorter than the previous case, in which the reference value of the wheel slip was a constant. Ten per cent improvement is achieved in the braking distance.

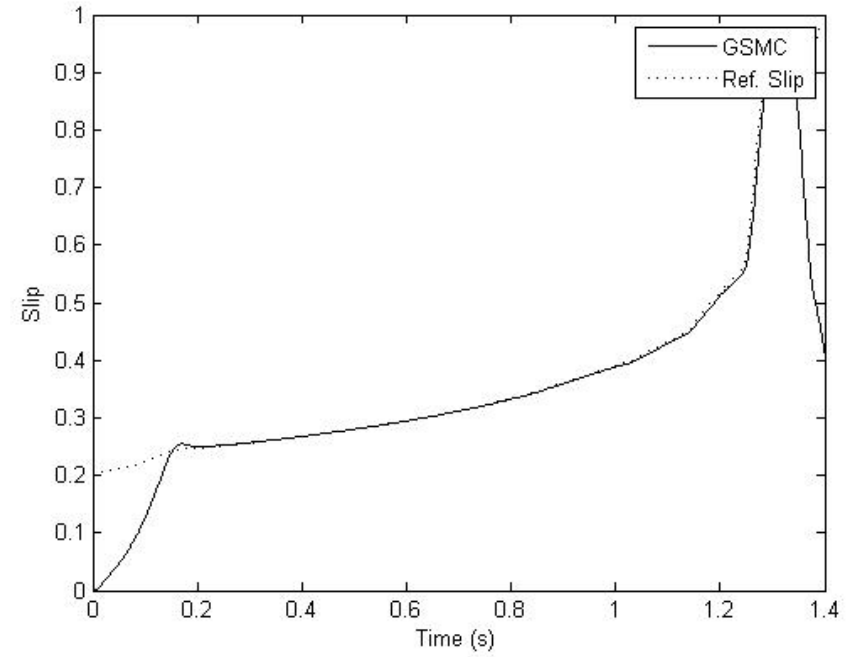

Figure 5.9. Wheel slip of SMC and GSMC for velocity dependent reference

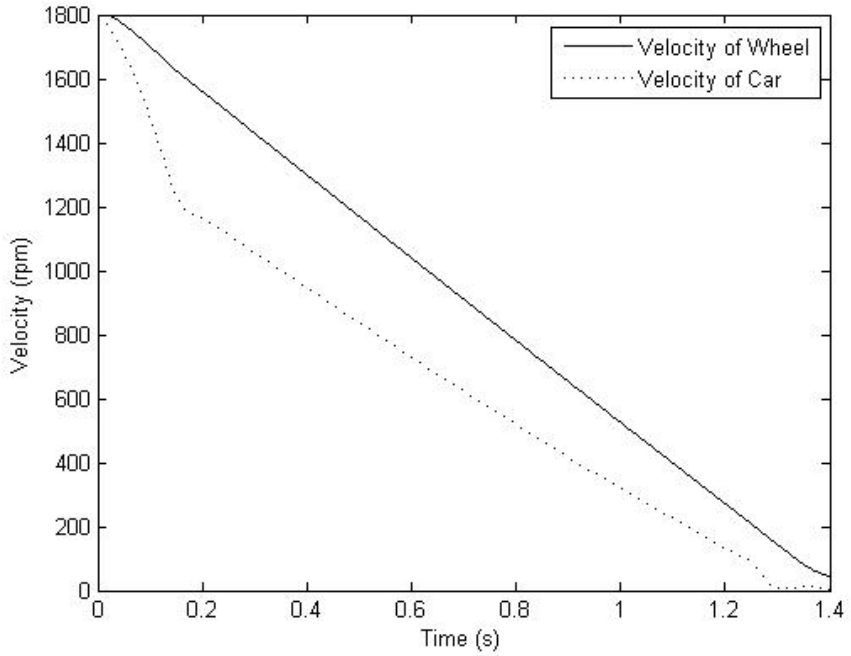

Figure 5.10. Wheel and vehicle velocities for velocity dependent reference

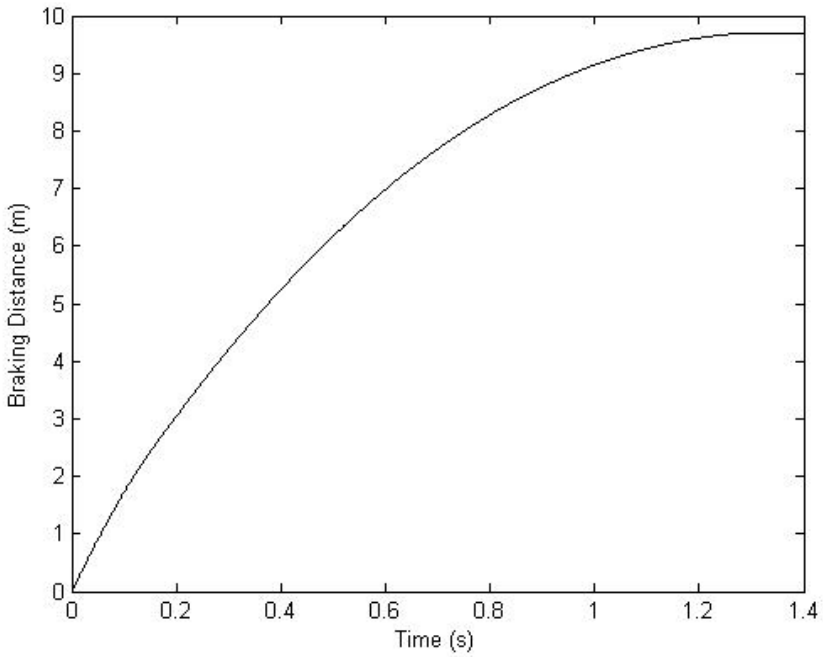

Figure 5.11. Braking distance of SMC and GSMC for velocity dependent reference

5.5. Experimental Results

A series of experiments have been conducted to determine the performance of the proposed controller for different cases and conditions. One of the parameters that has a deep impact on the effectiveness of controller is the step size of grey predictor. The step size should be selected appropriately, since if it is relatively large, it will cause over compensation resulting in a slow system response. On the other hand, if a small step size for the grey predictor is chosen, then the system will respond faster, but there may be overshoots. In the experiments, the step size of GSMC is set to 20. From Figure 5.12 to 5.15 present the system responses for constant and velocity dependent reference wheel slip values. The results of the experiments indicate that grey predictive controllers are robust in real-time systems that are subjected to noise from both inside and outside of the system.Although the magnitude of the fluctuations from the reference value is smaller for GSMC than SMC, both controllers exhibit similar performance. There is no drastic change either in stopping distance values between SMC and GSMC.

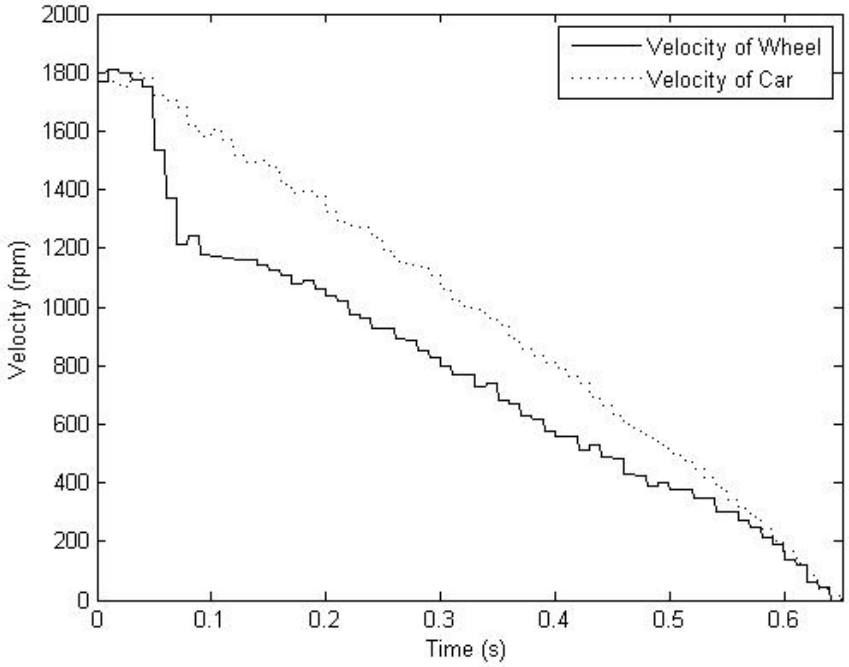

Figure 5.12. Experimental results of wheel and vehicle velocities for constant reference

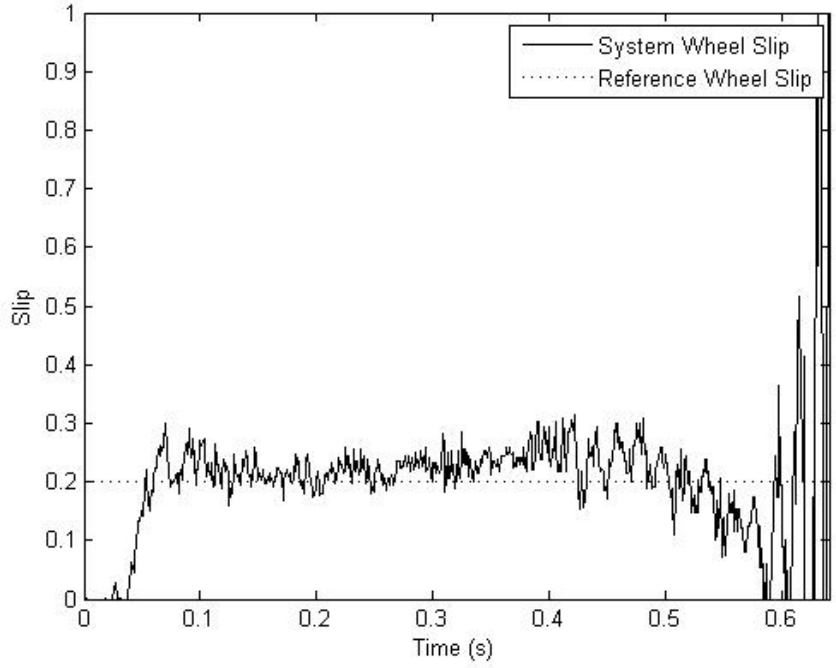

Figure 5.13. Experimental results of wheel slip for constant reference

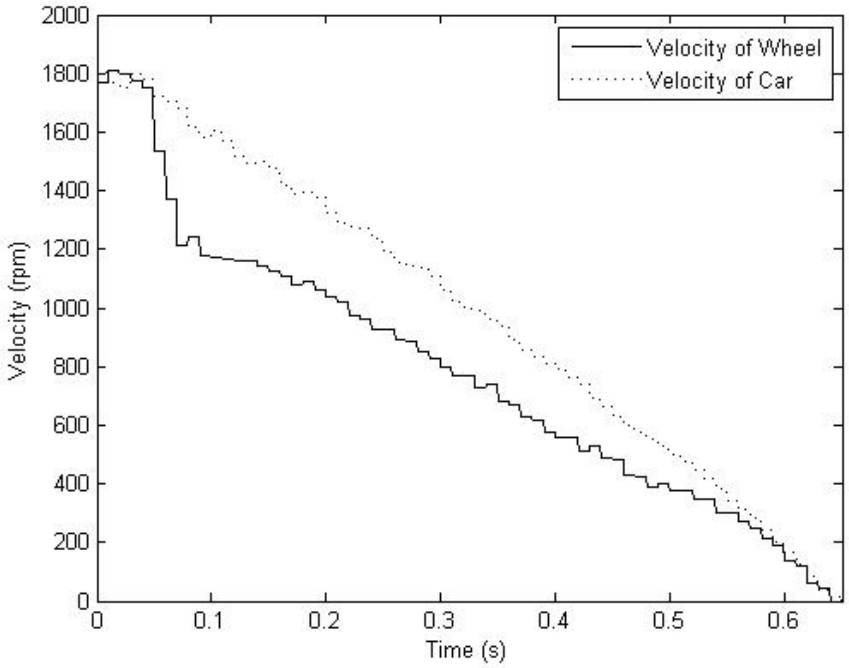

Figure 5.14. Experimental results of wheel and vehicle velocities for velocity dependent reference

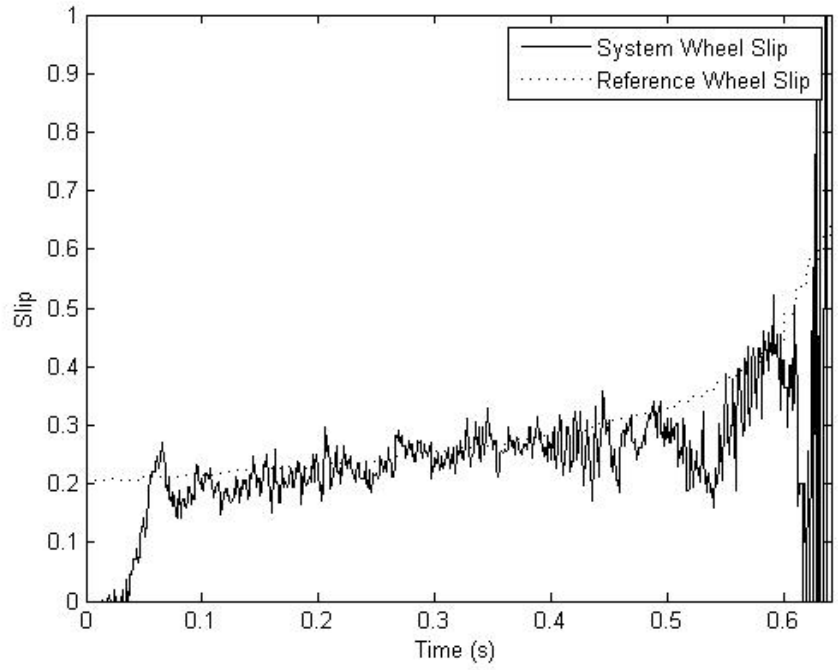

Figure 5.15. Experimental results of wheel slip for velocity dependent reference

5.6. Discussions

The underlying mathematics for grey system theory were explained in the previous chapter. Although Grey System Theory is a new emerging research field, it has already become popular among researchers because of its prediction capability. In this chapter, a grey sliding mode control algorithm for ABS system has been proposed. The grey prediction part of the controller anticipates the future outputs of the system using current data available. Based on the predicted values of wheel slip, SMC takes the necessary action to maintain the wheel at the desired value.

To investigate the performance of the proposed controller, the reference wheel slip is considered as both a constant value and a nonlinear function of the vehicle velocity. The results of simulations and experiments indicate that GSMC can handle uncertainties in the system, such as noisy measurements or disturbances. Hence, the braking operation will be more stable and the performance of ABS system will be increased.

6. CONCLUSIONS AND FUTURE WORK

In this thesis, the mathematical model of an ABS has been established and the control technique coupling grey predictor to sliding mode control has been designed. The choice of the sliding mode control and grey predictor stems from the nonlinear and uncertain characteristics of ABS. Sliding mode control is a robust control technique that is widely used in the control of nonlinear plants. Grey theory is a new emerging promising field for real time applications. Thus, it is assumed that a combination of these approaches may result in a more effective way to regulate the system of interest.

The main objective of the designed controller has been to maintain the wheel slip at a desired value such that the maximum braking power and maximum value of friction force between vehicle and road surfaces can be achieved. Two different approaches are employed to determine the reference value of wheel slip.

The effectiveness of both controllers is investigated through computer simulations and real-time experiments. The results of the simulations and experiments indicate that grey predictive controllers are, like SMC, robust in real-time systems that are subjected to noise from both inside and outsideu. It was expected that the combination of Grey prediction with SMC would result in a better performance. However, although some improvements in the noise response of the system are monitored, the GSMC exhibits similar results to SMC for this specific application. Some of the reasons for that may be that the assumptions made in the derivation of mathematical model and usage of a relatively simple model for the real-life system. Furthermore,the performance of the SMC is already excellent, which makes it difficult to design an outperforming controller.

Encouraged by the results of this study, further investigations on the topic for different road conditions are about to be launched. Moreover, in this thesis, it has been assumed that there is no interaction between four wheels but this is not the case in real life. In a further study, the interaction between these wheels can be taken into consideration.

APPENDIX A: MATLAB CODE USED IN SIMULATIONS


```
function  [sys,x0,str,ts] = sabs(t,x,u,flag,r1,r2,J1,J2,d1,d2,M10,M20,Mg,w,p,a,L,phi,u0,↙
b1,b2,tau,xini)
% S - function sabs
switch flag
    case 0  % Initialization
    sys = [3,  % number of continuous states
           0,      % number of discrete states
           7,    % number of outputs
           1,      % number of inputs
           0,      % reserved must be zero
           0,      % direct feedthrough flag
           1];     % number of sample times
    x0  = xini;
    str = [];
    ts  = [0 0];   % sample time: [period, offset]

    case 1                                                  % Derivatives
   % coefficients
        v1 = r1*x(1) ;
        v2 = r2*x(2) ;
        vr = r2*x(2)-r1*x(1) ;
        svr = sign(vr) ;
        s1 = tanh(x(1)) ;
        s2 = tanh(x(2)) ;
        M10 = s1*M10 ;
        M20 = s2*M20 ;
        sn = sin(phi) ;
        cn = cos(phi) ;
        c11 = r1*d1/J1 ;
        c12 = (M10+Mg)*r1/J1 ;
        c13 = -d1/J1 ;
        c14 = -M10/J1 ;
        c15 = r1/J1 ;
        c16 = -1/J1 ;
        c21 = -r2*d1/J2 ;
        c22 = -(M10+Mg)*r2/J2 ;
        c23 = -d2/J2 ;
        c24 = -M20/J2 ;
        c25 = -r2/J2 ;
        c31 = 1/tau ;
        ee = 1 ;
      rho = 1 ;
      nv = norm([v1 v2]) ;
      nve = nv/ee ;
        if nv<ee
            rho = (3-2*nve)*nve^2 ;
        end

   % slip
      if v2>=v1
         if (v1>0)&(v2>0)
            lam = (v2-v1)/(v2) ;
```

```
        elseif (v1<=0)&(v2>=0)
           lam = 1 ;
        elseif (v1<0)&(v2<=0)
           lam = (v1-v2)/(v1) ;
        end
     else
        if (v1>0)&(v2>0)
           lam = (v1-v2)/(v1) ;
        elseif (v1>=0)&(v2<=0)
           lam = 1 ;
        elseif (v1<=0)&(v2<0)
           lam = (v2-v1)/(v2) ;
        end
     end

     lam = lam*rho ;
       %krzywa tarcia
     lp = lam^p ;
       mu = w(4)*lp/(a+lp) ;
       mu = mu + w(3)*lam^3+w(2)*lam^2+w(1)*lam;
     mu = svr*mu ;
     mu = mu*rho ;

     % S(lam)
     S = (mu/L)/(sn-mu*cn) ;
     % hamulec

     if u>=u0
        b = b1*u+b2 ;
     else
        b = 0.0 ;
     end

     dx(1,1) = S*(c11*x(1)+c12)+c13*x(1)+c14+(c15*S+c16)*s1*x(3);
     dx(2,1) = S*(c21*x(1)+c22)+c23*x(2)+c24+c25*S*s1*x(3) ;
       dx(3,1) = c31*(b-x(3)) ;
     sys = dx;


   case 2                                                % Discrete state update
   sys = []; % do nothing

   case 3                                                                 % Outputs
  % coefficients
        v1 = r1*x(1) ;
        v2 = r2*x(2) ;
        vr = r2*x(2)-r1*x(1) ;
        svr = sign(vr) ;
        s1 = tanh(x(1)) ;
        s2 = tanh(x(2)) ;
        M10 = s1*M10 ;
        M20 = s2*M20 ;
```

```
        sn = sin(phi) ;
        cn = cos(phi) ;
        c11 = r1*d1/J1 ;
        c12 = (M10+Mg)*r1/J1 ;
        c13 = -d1/J1 ;
        c14 = -M10/J1 ;
        c15 = r1/J1 ;
        c16 = -1/J1 ;
        c21 = -r2*d1/J2 ;
        c22 = -(M10+Mg)*r2/J2 ;
        c23 = -d2/J2 ;
        c24 = -M20/J2 ;
        c25 = -r2/J2 ;
        c31 = 1/tau ;
        ee = 1 ;
        rho = 1 ;
      nv = norm([v1 v2]) ;
      nve = nv/ee ;
        if nv<ee
            rho = (3-2*nve)*nve^2 ;
        end

      % slip
      if v2>=v1
         if (v1>0)&(v2>0)
            lam = (v2-v1)/(v2) ;
         elseif (v1<=0)&(v2>=0)
            lam = 1 ;
         elseif (v1<0)&(v2<=0)
            lam = (v1-v2)/(v1) ;
         end
      else
         if (v1>0)&(v2>0)
            lam = (v1-v2)/(v1) ;
         elseif (v1>=0)&(v2<=0)
            lam = 1 ;
         elseif (v1<=0)&(v2<0)
            lam = (v2-v1)/(v2) ;
         end
      end
      lam = lam*rho ;
        %friction curve
      lp = lam^p ;
        mu = w(4)*lp/(a+lp) ;
        mu = mu + w(3)*lam^3+w(2)*lam^2+w(1)*lam;
      mu = svr*mu ;
      mu = mu*rho ;
      Fn = (s1*x(3)+M10+Mg+d1*x(1))/(L*sn-L*mu*cn) ;
      Ff = mu*Fn ;
      sys = [x(1:3);lam;abs(mu);Fn;Ff];

  case 9                                                % Terminate
```

```
    sys = []; % do nothing

  otherwise
    error(['unhandled flag = ',num2str(flag)]);
end
```

APPENDIX B: MATLAB CODE USED FOR GREY PREDICTION

22.08.2007 10:00 Block: ABS_greysim/Subsystem/Subsystem/grey predictor 1 of 1

```
function x_Predict = grey(x09, x08, x07, x06, x05, Clock)
step_size=20;

if (Clock < 0.005)
    x_Predict=x09;
else
    x11 = x05;
    x12 = x05+x06;
    x13 = x05+x06+x07;
    x14 = x05+x06+x07+x08;
    x15 = x05+x06+x07+x08+x09;

    B=[-(x11+x12)/2, 1 ; -(x12+x13)/2, 1 ; -(x13+x14)/2, 1 ; -(x14+15)/2, 1];
    Y=[x06, x07, x08, x09]';

    ab=inv(B'*B)*B'*Y;

    x_Predict =(x09-ab(2)/ab(1))*exp(-ab(1)*(step_size))*(1-exp(ab(1)));
end
```

REFERENCES

1. The Maintenance Council of the American Trucking Associations, *Technician Guidelines for Antilock Braking Systems*, Publication No. FHWA-MC-98-008, March 1998.

2. Hattori, Y., T. Takahashi, and A. Tanaka, "An Application of the Adaptive Method for the Sliding Mode Control of the Brake System", *The International Symposium on Advanced Vehicle Control*, Nagoya, pp.611-616, 1998.

3. Nice, K., *How Anti-Lock Brakes Work*, http://auto.howstuffworks.com/anti-lock-brake2.htm, 2007.

4. Harifi, A., A. Aghagolzadeh, G. Alizadeh and M. Sadeghi, "Designing a Sliding Mode Controller for Antilock Brake System", *The International Conference on Computer as a Tool* , Serbia and Montenegro, pp.611-616, 2005 .

5. Zanten, A., R. Erhardt and A. Lutz, "Measurement and Simulation of Transients in Longitudinal and Lateral Tire Forces", *SAE Paper 900210*, vol. 99, no. 6, pp. 300-318, 1990.

6. Svendenius, J., *The Tire Models for Use in Braking Applications*, Department of Automatic Control, Lund Institute of Technology, Sweden, 2003.

7. Akbarzadeh,M. R., K. J. Emami and N. Pariz, "Adaptive Discrete-Time Fuzzy Sliding Mode Control for Anti-Lock Braking Systems", *in Annual Meeting of the North American*, New Orleans, USA, pp. 554-559, 2002.

8. Veloso,F. and S. K. Fixson, "Make-Buy Decisions in the Auto Industry: New Perspectives on the Role of the Supplier as an Innovator", *Technological Forecasting and Social Change*, vol. 67, pp. 239-257, 2001.

9. Limpert,R., *Brake Design and Safety*, Society of Automotive Engineers Inc., Second Edition, USA, 1999.

10. "The World of ABS", *25th Bosch ABS Anniversary*, http://www.bosch.com/content/language2/html/2329.htm, 2007.

11. Lin, W. C. and Y. K. Chin, *Variable-Structure Brake Control for Anti-skid and Anti-spin*, Report No. EG-275, General Motors Research Laboratories, Warren, Michigan, 1986.

12. Tan, H. S. and M. Tomizuka, "An Adaptive and Robust Vehicle Traction Controller Design", *in Proceedings of American Control Conference*, Pittsburgh, PA, pp. 1053-1058, 1989.

13. Chin, Y. K., W. C. Lin, D. M. Sidlosky and M. S. Sparschu, "Sliding-mode ABS Wheel Slip Control", *in Proceedings of American Control Conference*, Chicago, USA, pp 1-6, 1992.

14. Drakunov, S., U. Ozguner, P. Dix and B. Ashrafi, "ABS Control Using Optimum Search Via Sliding Modes", *IEEE Transactions on Control Systems Technology*, vol. 3, No 1, pp. 79-85, 1995.

15. Kachroo, P. and M. Tomizuka, "Sliding Mode Control with Chattering Reduction and Error Convergence for a Class of Discrete Nonlinear Systems with Application to Vehicle Control", *International Mechanical Engineering Congress and Expo, ASME 1995 Meeting*, DSC-Vol. 57-1, pp. 225-233, 1995.

16. Unsal, C. and P. Kachroo, "Sliding Mode Measurement Feedback Control for Antilock Braking Systems", *IEEE Transactions on Control Systems Technology*, vol. 7, No. 2, pp. 271-281, 1999.

17. Schinkel, M. and K. Hunt, "Anti-Lock Braking Control using a Sliding Mode Approach", *Proceedings of the 2002 American Control Conference*, Anchorage, Alaska,

8-10 May 2002, pp. 2386-2391, 2002.

18. Mauer, G. F., "A Fuzzy Logic Controller for an ABS Braking System", *IEEE Transactions on Fuzzy System*, Vol. 3, No. 4, pp. 381-388, 1995.

19. Layne, J. R., K. M. Passino and S. Yurkovich, "Fuzzy learning control for antiskid braking systems", *IEEE Transaction on Control System Technology*, Vol. 1, No. 2, pp. 122-129, June 1993.

20. Will, A. B., S. Hui and S. H. Zak, "Sliding Mode Wheel Slip Controller for an Antilock Braking System", *International Journal of Vehicle Design*, Vol. 19, No. 4, pp. 523-539, 1998.

21. Lee, Y. and H. S. Zak, "Genetic Neural Fuzzy Control of Anti-Lock Brake Systems", *Proceedings of the 2001 American Control Conference*, Arlington, Virginia, 25-27 June 2001, Vol. 2, pp. 671-676, 2001.

22. *The Laboratory Antilock Braking System Controlled from PC*, User's Manual, Inteco Ltd., Poland, 2006.

23. Olsson, H.,*Control Systems with Friction*, Ph.D. Thesis, Lund Institute of Technology, 1996.

24. Yi, J., L. Alvarez, R. Horowitz and C. Canudas, "Adaptive emergency braking control based on a tire/road friction dynamic model", *Proceedings of the 39th Conference on Decision and Control*, Sidney, December 2000, Vol. 1, pp. 456-461, 2000.

25. Ming, Q., *Sliding Mode Controller Design for ABS System*, M.S. Thesis, Virginia Polytechnic Institute and State University, 1997.

26. V. Utkin, J. Guldner and J. Shi, *Sliding Mode Control in Electromechanical Systems*, Taylor & Francis Inc., Philadelphia, USA, 1999.

27. Zak, S. H., *Systems and Control*, Oxford University Press, New York, 2003.

28. Slotine, J. J. E and W. Li, *Applied Nonlinear Control*, Englewood Cliffs, Prentice Hall, New Jersey, 1991.

29. DeCarlo, R.A., S. H. Zak, and G.P. Matthews, "Variable Structure Control of Nonlinear Multivariable System: A Tutorial", *Proceedings of the IEEE*, Vol. 76, No. 3, pp. 212-232, 1988.

30. Schmidtbauer, B., *Modellbaserade Reglersystem*, Studentlitteratur, Lund, Sweden, 1999.

31. Patil, C.B., *Antilock Brake System Re-design and Control Protoyping Using a One-Fifth Scale Vehicle Experimental Test Bed*, M.S. Thesis, University of Texas, 2003.

32. C. Edwards and S. K. Spurgeon, *Sliding Mode Control Theory and Applications*, Taylor and Francis Ltd., USA, 1998.

33. Buckholtz, K. R., "Reference Input Wheel Slip Tracking Using Sliding Mode Control", *in SAE 2002 World Congress*, Detroit, Michigan, Report No. 2002-01-0301, 2002.

34. Lee, J. H., P. U. Allire, G. Tao, J. A. Decker and X. Zhang, "Experimental Study of Sliding Mode Control for a Benchmark Magnetic Bearing System and Artificial Heart Suspension", *IEEE Transaction on Control System Technology*, Vol. 11, pp. 128-138, 2003.

35. Deng, J. L., "Control Problems of Grey System", *System and Control Letters*, Vol. 1, No. 5,pp. 288-294, 1982.

36. Liu, S. F. and Y. Lin, *Collected Papers on Grey Systems*, Press of Henna University, Kaifeng, 1993.

37. Cheng, B., "The Grey Control on Industrial Process", *Journal of Huangshi College*, Vol. 1, pp. 11-23, 1986.

38. Luo, J. J. and B. X. Zhang, "A Study of Grey Forecasting and its Control Analysis of Grain Yield", *The Journal of Grey Systems*, Vol. 1, No. 1, pp. 91-98, 1989.

39. Tamura, Y., D. P. Zhang, U. Umeda and K. Sakashit, "Load Forecasting Using Grey Dynamic Model", *The Journal of Grey Systems*, Vol. 4, No. 1, pp. 45-48, 1992.

40. Song, S. Y., "The Application of Grey system Theory to Earthquake Prediction in Jiangsu Area", *The Journal of Grey Systems*, Vol. 4, No. 4, pp. 359-367, 1992.

41. Hong, C. M., S. C. Lin and C. T. Chiang, "Control of Dynamic Systems by Fuzzy-based Grey Prediction Controller", *The Journal of Grey Systems*, Vol. 7, No. 1, pp. 23-44, 1995.

42. Huang, S. J. and C. L. Huang, "Control of an Inverted Pendulum Using Grey Prediction Model", *IEEE Transactions on Industry Applications*, Vol. 36, No. 2, pp. 452-458, 1994.

43. Huang, Y. P. and S. F. Wang, "Identifying the Fuzzy Grey Prediction Model by Genetic Algorithms", *Proceedings of the 1996 IEEE International Conference on Evolutionary Computation*, Nagoya, Japan, May 1996, pp. 720-725, 1996.

44. Wong, C. C. and C. C. Chen, "Design of Fuzzy Control Systems with a Switching Grey Prediction", *Proceedings of the 1998 IEEE International Conference on Fuzzy Systems*, Anchorage, USA, May 1998, Vol. 1, pp. 567-571, 1998.

45. Lin, K. H. and B. D. Liu, "Design of Predictive Fuzzy Control System Using GESA-Based Grey Predictor", *Journal of the Chinese Institute of Engineers*, Vol. 10, No.2, pp. 145-154, 2002.

46. Lin, Y. and S. Liu, "A Historical Introduction to Grey Systems Theory", *Proceedings of the 2004 IEEE International Conference on Systems, Man and Cybernetics*, Vol. 3, pp. 2403- 2408, 2004.

47. Liu, S. F. and Y. Lin, *An Introduction to Grey Systems*, IIGSS Academic Publisher,

PA, USA, 1998.

48. Kayacan, E., *Grey Prediction Based Control of a Non-linear Liquid Level System Using PID Type Fuzzy Controller*, M. S. Thesis, Boğaziçi University, 2006.

49. Wong,C. C. and C. C. Chen, "Gain Scheduling of Grey Prediction Fuzzy Control Systems", *International Journal of Fuzzy Systems*, Vol. 2, No.3, pp. 198-204, 2000.

50. Deng, J. L., Introduction to Grey System Theory, *The Journal of Grey System*, vol. 1, pp. 1-24, 1989.

51. Lu, H. C., "Grey Prediction Approach for Designing Grey Sliding Mode Controller", *in IEEE International Conference on Systems, Man and Cybernetics*, Netherlands, pp. 403-408, 2004.